A novel proteinaceous molecule produced by *Lysinibacillus* sp. OF-1 depends on the Ami oligopeptide transporter to kill *Streptococcus pneumoniae*.

Ingvild Hals Hauge[1], Vilde Sandegren[1], Anja Ruud Winther[1], Cathrine Arnason Bøe[2], Zhian Salehian[1], Leiv Sigve Håvarstein[1], Morten Kjos[1] and Daniel Straume[1]*.

[1]Faculty of Chemistry, Biotechnology and Food Science, Norwegian University of Life Sciences, 1430 Ås, Norway.

[2]Norwegian Veterinary Institute, Department of Molecular Biology, 1433 Ås, Norway.

Running title: Lysinicin OF, a novel antimicrobial molecule.

Key words: *Lysinibacillus*, antimicrobials, *Streptococcus pneumoniae*, lysinicin OF

*Corresponding author:
Daniel Straume
Faculty of Chemistry, Biotechnology and Food Science
Norwegian University of Life Sciences
1430, Ås, Norway
daniel.straume@nmbu.no, +47 67232560

Abstract.

Infections caused by antibiotic resistant *Streptococcus pneumoniae* are of growing concern for the healthcare systems who need new treatment options. Screening microorganisms in terrestrial environments have proved successful for discovering antibiotics, while production of antimicrobials by marine microorganisms remains underexplored. Here we have screened microorganisms sampled from the Oslo Fjord in Norway for production of molecules that prevent the human pathogen *S. pneumoniae* from growing. A bacterium belonging to the genus *Lysinibacillus* was identified. We show that this bacterium produces a molecule that kills a wide range of streptococcal species. Genome mining in BAGEL4 and AntiSmash suggested that it was a new antimicrobial compound, and we therefore named it lysinicin OF. The compound was resistant to heat (100°C) and polymyxin acylase but susceptible to proteinase K, showing that it is of proteinaceous nature, but most probably not a lipopeptide. *S. pneumoniae* became resistant to lysinicin OF by obtaining suppressor mutations in the *ami* locus, which encodes the AmiACDEF oligo peptide transporter. We created Δ*amiC* and Δ*amiEF* mutants to show that pneumococci expressing a compromised Ami-system were resistant to lysinicin OF. Furthermore, by creating mutants expressing an intact but inactive Ami-system (AmiED184A and AmiFD175A) we could conclude that the lysinicin OF activity depended on the active form (ATP-hydrolysing) of the Ami-system. Microscopic imaging and fluorescent labelling of DNA showed that *S. pneumoniae* treated with lysinicin OF had an average reduced cell size with condensed DNA nucleoid, while the integrity of the cell membrane remained intact. The characteristics and possible mode of actions of lysinicin OF are discussed.

Introduction.

The growing numbers of antibiotic resistant pathogens are a global concern threatening several aspects of modern medicine (1, 2). Efficient antibiotics are critical not only to treat bacterial infections in general, but also to prevent infections after surgeries and in patients undergoing chemotherapy. Efforts to slow down the spread of antibiotic resistance among pathogens include restrictive use of antibiotics by the medical healthcare systems as well as in the agricultural industry. Combined with vaccination programs and the use of narrow range antibiotics, the spreading of antibiotic resistance can be slowed down. However, these measures do not offer a final solution to the problem. Therefore, to have treatment options for bacterial infections in the future, there is a need to discover new antimicrobial compounds with the potential of clinical use. *Streptococcus pneumoniae*, also called pneumococcus, is a human pathogen causing pneumonia, bacteremia, meningitis and otitis media (3). Children, elderly, and immunocompromised individuals are particularly susceptible of being infected with pneumococci. Penicillin is the antibiotic of choice, but its clinical relevance is fading due to increasing numbers of infections caused by penicillin resistant strains. In addition, several pneumococcal isolates are reported to be resistant to macrolides, fluoroquinolones and tetracyclines (4). Since *S. pneumoniae* can become competent for natural genetic transformation, the resistance genes can be rapidly spread to susceptible strains, adding an extra layer to this challenge (5).

In this work we set out to find new natural compounds that inhibited growth of *S. pneumoniae*. A large number of antibiotics used today, e.g. β-lactams, macrolides and tetracyclines, are natural products produced by other microorganisms found in terrestrial habitats (6, 7). Production of antimicrobials by marine microorganisms, however, is underexplored. Therefore, we sampled microorganisms from the shore of the Oslo Fjord in Norway and screened them for production of anti-pneumococcal activity. Here we describe an

isolate belonging to the genus *Lysinibacillus* that produces a novel compound inhibiting *S. pneumoniae* and other streptococcal species. We show that this compound, which we named lysinicin OF, depends on the Ami oligopeptide uptake system to kill *S. pneumoniae* by an unknown mechanism. The biophysical properties and mode of action of lysinicin OF are discussed.

Material and Methods.

Bacterial strains, growth conditions and transformation.

All bacterial species and mutants used in this study are listed in Table S1. *S. pneumoniae* was grown in liquid C medium (8) without shaking and on Todd Hewitt (TH)-agar (Becton, Dickinson and Company) at 37°C. Other streptococcal species were grown in TH broth and on TH agar. When grown on TH agar, all streptococci were incubated anaerobically by placing them in an airtight container containing AnaeroGenTM bags from Oxoid. Growth curves of pneumococcal strains were obtained by growing them in 96-well microtiter plates using a Hidex Sense Microplate Reader. All strains were pre-grown for one hour in C medium before they were diluted to OD_{550} = 0.05 in fresh C medium and transferred to a microtiter plate. In some cases, a final concentration of 2 µM Sytox Green™ (ThermoFisher Scientific) was added to the wells for detection of cell lysis. Sytox Green fluoresces upon DNA binding, to which it gets access only if the cell membrane integrity is disrupted. Sytox Green™ was excited at 485 nm and the light emission at 535 nm was measured. *Escherichia coli* was grown in Lysogeny broth (LB) with shaking. *Bacillus subtilis*, *Staphylococcus aureus*, *Pseudomonas brenneri* and *Mycobacterium smegmatis* were grown in brain heart infusion (BHI) broth (Oxoid). *B. subtilis*, *S. aureus* and *M. smegmatis* were incubated at 37°C with shaking, while *P. brenneri* was incubated at 22°C without shaking. *Lactococcus lactis* was grown in GM17 (Oxoid) at 30°C

97 without shaking, and *Enterococcus faecalis* was grown in BHI at 37°C without shaking.
98 *Lysinibacillus* sp. OF-1 was grown aerobically in TH broth, in M9 medium (supplemented with
99 a final concentration of 0.4% (v/v) glucose, 10 µg/ml (w/v) of all 20 amino acids, 1 mM
100 $MgSO_4$, 0.1 mM $CaCl_2$ and 1 µg/ml (w/v) thiamine) and on TH agar at room temperature.
101 Liquid cultures of *Lysinibacillus* sp. OF-1 were grown without shaking, but a maximum liquid
102 depth of 3 cm allowed sufficient aerobic conditions.

103 *S. pneumoniae* was transformed by mixing one ml of exponentially growing cells
104 (OD_{550} between 0.05 and 0.1) with 100-200 ng of transforming DNA and CSP-1 (final
105 concentration of 250 ng/ml). The transforming cells were incubated at 37°C for two hours
106 before 30 µl of the cell culture were plated on TH agar containing a final concentration of 400
107 µg/ml kanamycin, 200 µg/ml streptomycin, 200 µg/ml spectinomycin or 2.5 µg/ml
108 chloramphenicol.

109

110 **Sampling and soft-agar overlay assay.**

111 Samples were collected from the Oslo Fjord at the shore near a small village called Hvitsten.
112 Samples from rocks, seaweed, sand, mud, and seawater were spread onto BHI-, LB-, TH- and
113 Miller Hinton agar (Becton, Dickinson and Company) and incubated at room temperature for
114 five days to obtain bacterial colonies. A volume of 100 µl *S. pneumoniae* culture with OD_{550} =
115 0.3 was added to five ml of melted TH soft-agar (0.75 % [w/v] agar) holding 47°C. The soft-
116 agar was then mixed by vortexing for two seconds, before it was gently spread on top of
117 colonies formed by the marine bacteria as described above. After anaerobic incubation at 37°C
118 over-night, the plates were inspected for colonies surrounded by inhibition zones. For detection
119 of inhibition zones surrounding *Lysinibacillus* sp. OF-1 colonies, the same protocol with TH-
120 soft-agar was used for all streptococcal indicator species. BHI soft-agar was used when *P.*

brenneri, *B. subtilis*, *S. aureus* an *M. smegmatis* were the indicators, while LB-soft-agar was used for *E. coli* and GM17 soft-agar for *L. lactis* and *E. faecalis*.

DNA techniques.

All primers used for PCR are listed in Table S2. Gene cassettes used for transformation of *S. pneumoniae* were created by overlap extension PCR (9). To make gene deletion cassettes, the ~1000 bp regions upstream and downstream of a gene of interest were fused to the 5' and 3' end of a desired antibiotic resistance gene (Kan^r, Spc^r, Cam^r). A Janus cassette (10) was used to introduce gene deletions or mutations. When appropriate the Janus was replaced through negative selection with a DNA sequence of interest by fusing it with the same ~1000 bp regions flanking the Janus. Point mutations and fusion tags were introduced by primer design and overlap extension PCR.

Lysinicin OF enrichment.

Lysinibacillus sp. OF-1 was cultivated for four days in 500 ml TH broth. Cells were removed by centrifugation at 5000 x *g*, and the supernatant was transferred to an Erlenmeyer flask containing three grams of Amberlite® XAD16N 20-60 mesh beads (Sigma). The flask was incubated at room temperature with shaking for one hour. The beads were then washed twice with water, once with 20% ethanol before the remaining material bound to the beads was eluted by 3x5 ml 96% ethanol. The three elution fractions were pooled and dried by vacuum centrifugation. The dried material was dissolved in one ml sterile water and stored at -20°C.

Whole genome sequencing and genome analyses.

Genomic DNA from bacteria was isolated by using NucleoBond® AXG100 columns as described in the included protocol from Macherey-Nagel. Re-sequencing of gDNA from pneumococcal mutants was performed by using MiSeq nano v2 with paired ends reads of 250 bp yielding approximately 35x coverage. Genomic DNA from *Lysinibacillus* sp. OF-1 was subjected to both short (Illumina) and long read (Nanopore) sequencing. Illumina sequencing of *Lysinibacillus* sp. OF-1 was performed using v3 chemistry on the MiSeq with paired end reads of 300 bp yielding 80x coverage. For long read sequencing a library was prepared from 400 ng of gDNA using the Rapid Barcoding Kit SQK-RBK004 from Oxford Nanopore Technologies. This library was further sequenced on the MinION sequencer using the FLO-Min106D flowcell (Oxford Nanopore Technologies). Fast5 files generated from nanopore sequencing were used for basecalling with Guppy (version 4.0.15). Quality control of the sequencing run was performed with NanoPlot (Version: 1.33.1). Fastq files from nanopore sequencing were demultiplexed with Qcat (version 1.1.0), where barcodes were trimmed, and reads shorter than 50 bp were excluded. The demultiplexed fastq files were then processed with NanoFilt (version 2.7.1) to remove reads with a Phred score quality lower than seven, a minimum length below 100 bp. In addition, the first 50 bp of all reads were removed using the headcrop option. *de novo* assembly of the *Lysinibacillus* sp. OF-1 genome was done by hybrid assembly of the Illumina and Nanopore sequences using the Ellipsis pipeline (10.5281/zenodo.4563897). Annotation of the *Lysinibacillus* sp. OF-1 genome was done using prokka 1.14.5 (11).

Microscopic analyses.

For microscopic imaging, bacteria were immobilized on a thin layer (<0.5 mm) of 1.2 % (w/v) agarose in PBS. Phase contrast and fluorescence pictures were taken by using a Zeiss AxioObserver with ZEN Blue software, an ORCA-Flash 4.0 V2 Digital CMOS camera (Hamamatsu Photonics), and a 100x phase-contrast objective. An HXP 120 Illuminator (Zeiss) served as light source for fluorescence microscopy. To stain bacterial nucleoids, cells were treated with a final concentration of 0.2 µg/ml 4′,6-diamidino-2-phenylindole (DAPI) for five minutes prior to imaging. For live/dead staining (Live/Dead® *Bac*Light™, Thermofisher Scientific) three µl of a 1:1 mixture of Propidium iodide (20 mM) and Syto® 9 (3.34 mM) were added to one ml cell culture followed by incubation for 15 minutes in the dark before imaging. Images were analysed using the ImageJ software with the MicrobeJ plugin (12).

Immunoblotting.

Pneumococcal mutants were grown to OD_{550} = 0.25 in 10 ml volumes. Cells were harvested at 4000 x *g* and lysed in 200 µl SDS sample buffer at 95 °C for 5 minutes. Total protein extracts from 15 µl samples were separated by SDS-PAGE using a 12% separation gel and the protocol of Laemmli (13). Proteins were transferred onto a PVDF membrane using the Trans-Blot Turbo Transfer System from BioRad. Flag-tagged proteins were detected as described by Stamsås et al (14) using the polyclonal anti-Flag antibody (Sigma, cat. F7425) and horse radish peroxidase conjugated anti-rabbit (Thermo Fisher, cat. 31460) as secondary antibody. Both antibodies were diluted 1:4000 in TBS-T.

Hemolysis assay.

Sheep blood (Thermo Fisher) was first diluted 1:9 in PBS before erythrocytes were collected at 1500 x *g* for 10 min. The erythrocytes were then washed twice in PBS and finally resuspended in a volume of PBS resulting in a 1:9 dilution of the blood. Aliquots of 990 µl diluted blood were transferred to Eppendorf tubes containing 10 µl lysinicin OF (final concentration of 10xMIC), 10 µl Triton X-100 (final concentration of 1 % [v/v]) or 10 µl PBS. The blood samples were incubated at 37°C for 30 min. Next, intact erythrocytes were removed from the solution at 1500 x *g* for 10 min and Abs490 of the supernatants were measured.

Spot-assay.

Exponentially growing *S. pneumoniae* at OD_{550} = 0.2 were treated with 10xMIC lysinicin OF (10 µl/ml), rifampicin (0.39 µg/ml), ciprofloxacin (12.5 µg/ml), ampicillin (3.1 µg/ml) or tetracycline (3.1 µg/ml) for 30 minutes before the cells were washed three times in fresh C medium. Next, the cells were resuspended in C medium to OD_{550} = 0.1 and diluted in a 10-fold dilution series of C medium. Three µl of the dilutions 10^{-1} – 10^{-6} were spotted on TH agar. When the spotted dilutions had dried, the plate was incubated at 37°C for 18 hours.

Results.

A *Lysinibacillus* isolate showed antimicrobial activity against *S. pneumoniae*.

We wanted to explore if bacteria from the marine habitat have the potential to produce novel antimicrobial compounds against *S. pneumoniae*. Bacteria were sampled from the shore in the Oslo Fjord, including rocks, sand, mud, seaweed, and seawater. The samples were plated on Todd-Hewitt, brain heart infusion, Luria Bertani and Muller Hinton media and incubated

aerobically at room temperature for five days. To screen for antimicrobial activity against *S. pneumoniae*, the RH425 strain (R6 derivate) was included in TH soft-agar placed on top of the marine bacteria. After anaerobic incubation overnight, RH425 inhibition zones were identified. One bacterial colony sampled from the surface of a rock showed a particularly large inhibition zone on TH agar (Fig. S1). A pure culture of this bacterium was obtained and a new soft-agar overlay assay was performed to verify the inhibition of *S. pneumoniae* (Fig. 1A). Indeed, this marine bacterium displayed strong inhibition of *S. pneumoniae*. To identify the isolate, we sequenced its genome and used the 16S rRNA sequence in a BLASTn search. The best hits were *Lysinibacillus sphaericus* KCCM 35418 and *L. fusiformis* NEB 1292 (100% and 99.87 % identity), both belonging to the *Bacillaceae* family. Pair-wise genome sequence alignments using BLAST2 showed that the KCCM 35418 genome covered 77% of the marine isolate's genome with a nucleotide identity of 93.09%, while the NEB 1292 genome showed 80% coverage with 95.36% nucleotide identity. This shows that the isolate is closely related to *L. sphaericus* and *L. fusiformis*, but also that a large portion of its genetic content is not found in these species. The *Lysinibacillus* genus currently holds 23 species (NCBI taxonomy ID 400634). To place the isolate in this genus, a phylogenetic tree was generated (Fig. S2) by using the M1CR0B1AL1Z3R tool (15) and a selection of 31 genome sequences from the NCBI GeneBank, including all 23 *Lysinibacillus* species. The phylogram placed the *Lysinibacillus* isolate on the same clade as *L. fusiformis* NEB 1292 confirming a close evolutionary relationship between these two bacteria. However, based on the 16S rRNA and genome sequence analyses (77-80% coverage) it was difficult to distinguish whether the isolate was an *L. fusiformis* or an *L. sphaericus*, and we have therefore named it *Lysinibacillus* sp. strain OF-1 (for Oslo Fjord isolate 1). It has a genome size of 4 710 095 nucleotides with a GC content of 37.8% (accession number in GenBank: CP102798). Annotation using prokka 1.14.5 (11)

predicted 4658 genes. *Lysinibacillus* sp. OF-1 is a typical rod-shaped bacillus that frequently formed endospores when grown on TH agar (Fig. 1B).

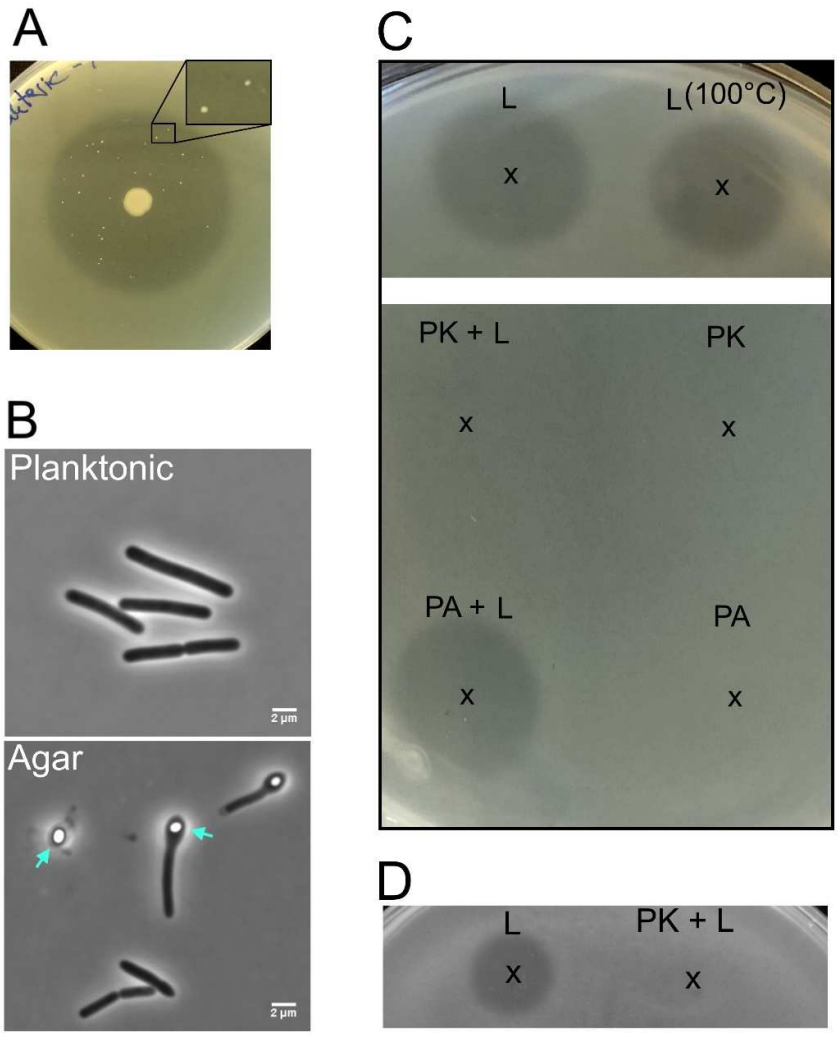

Fig. 1. *Lysinibacillus* sp. OF-1 produces a proteinaceous compound that inhibits *S. pneumoniae*. (A) A colony of *Lysinibacillus* sp. OF-1 overlayed with TH soft-agar containing *S. pneumoniae*. Growth inhibition of *S. pneumoniae* is seen as a clear zone surrounding the *Lysinibacillus* sp. OF-1 colony. Several resistant pneumococcal mutants emerged in the inhibition zone after prolonged (48 hours) incubation at 37°C (zoomed panel). (B) Phase contrast images of *Lysinibacillus* sp. OF-1 grown in liquid culture (planktonic) and over-night on TH agar. Endospores are indicated by arrows. Scale bars are 2 µm. (C) *S. pneumoniae*-containing soft-agar on which three µl of lysinicin OF (L) exposed to different treatments were spotted (indicated by x). Lysinicin OF was either incubated at 100°C for 30 min, incubated with 500 µg/ml proteinase K (PK + L) or 50 µg/ml polymyxin acylase (PA + L). Proteinase K and polymyxin acylase (PK and PA) had no inhibitory effect on their own. (D) Activity of nontreated and proteinase K treated lysinicin OF extracted from culture supernatants of *Lysinibacillus* sp. OF-1 grown in minimal M9 medium.

Lysinibacillus sp. OF-1 produces a proteinaceous compound that kills *S. pneumoniae* and other streptococci.

To identify *Lysinibacillus* sp. OF-1 gene clusters potentially involved in the production of already known antimicrobial compounds genome mining was done using BAGEL4 (16) and AntiSMASH 6.1.1 (17). BAGEL4 is used to identify biosynthetic gene clusters involved in production of RiPPs (ribosomally synthesized and posttranslationally modified peptides) while AntiSMASH in addition finds gene clusters involved in synthesis of other secondary metabolites with known antimicrobial activity. No clear hits were found with BAGEL4, whereas AntiSMASH gave a similarity hit of 46% (percent genes found in known gene clusters) to a gene cluster in *B. velezensis* FZB42 responsible for synthesis of the cyclic lipopeptide fengycin (Fig. S3). However, the *Lysinibacillus* sp. OF-1 genome lacks the *fenABCDE* genes (fengycin synthetase A-E) (18), strongly suggesting that the bacterium does not produce a fengycin-like molecule.

To examine the physico-biochemical properties of the antimicrobial compound produced by *Lysinibacillus* sp. OF-1, we first tried to concentrate it from culture supernatants by using hydrophobic XAD Amberlite 16N beads (see material and methods). Indeed, the material eluted from the XAD beads inhibited *S. pneumoniae* (Fig. 1C), demonstrating hydrophobic properties of the compound. Since species belonging to the *Bacillus* genus often produce antimicrobial proteins, peptides and lipopetides (19, 20), we tested how proteinase K, polymyxin acylase and heat treatment would affect the antimicrobial activity of the compound. Neither heat treatment at 100°C for 30 minutes nor incubation with polymyxin acylase (cleaving the acyl bond between the peptide and lipid part of lipopeptides) reduced its antimicrobial effect on *S. pneumoniae*. Treatment with proteinase K on the other hand completely inactivated the antimicrobial activity (Fig. 1C). This demonstrated that the antimicrobial compound is of proteinaceous nature but most likely not a lipopeptide.

279 Considering that it retained inhibitory activity after 100°C for 30 minutes, we reasoned that the
280 compound could be a peptide or possibly a glycopeptide. The latter seemed less likely since
281 antimicrobial glycopeptides (e.g., vancomycin, teicoplanin and balhimycin) are usually
282 produced by bacteria belonging to Actinomycetia (21) and that we did not find glycopeptide
283 gene clusters in the *Lysinibacillus* sp. OF- 1 genome. We named the compound lysinicin OF.
284 To confirm that lysinicin OF was produced by *Lysinibacillus* sp. OF-1 and not a degradation
285 product derived from consumption of the TH-medium, we also successfully enriched the
286 compound from the supernatant of *Lysinibacillus* sp. OF-1 grown in M9 mineral medium
287 supplemented with amino acids (see methods) (Fig. 1D). By using UHPLC and MALDI TOF
288 MS-MS, we have made several attempts to identify the mass and amino acid composition of
289 the lysinicin OF extracted from both TH and M9 medium, however, thus far none have been
290 successful. For HPLC-fractionated TH supernatants, we found only peptides deriving from the
291 growth medium, while in M9 supernatants we obtained many peaks of different masses. We
292 were not able to pinpoint which of the masses that represented the active compound.

293 To determine whether lysinicin OF had a target range beyond the pneumococcus, we
294 performed soft-agar overlay assays using a selection of streptococci covering species from all
295 six streptococcal sub-groups (Mitis, Pyogenes, Anginosus, Mutans, Bovis and Salivarius) as
296 well as more distantly related species such as *M. smegmatis*, *B. subtilis*, *S. aureus*, *L. lactis*, *E.*
297 *faecalis*, *P. brenneri* and *E. coli* as indicators. The results are presented in Table 1 (see Fig.
298 S4A for overlay assays). All streptococci tested displayed various degrees of sensitivity to
299 lysinicin OF, except for *S. agalactiae* NCTC8181 from the pyogenes group, which had no
300 inhibition zone. However, another representative from the pyogenes group, *S. phocae*
301 ATCC29128, was sensitive, showing that species within all six subgroups of streptococci were
302 sensitive to lysinicin OF. In addition, lysinicin OF displayed weak inhibitory effect against *B.*
303 *subtilis*, but not against *M. smegmatis*, *S. aureus*, *L. lactis*, *E. faecalis*, *P. brenneri* and *E. coli*.

Table 1. Bacteria tested for lysinicin OF sensitivity in soft-agar overlay assays.

Species	Sensitive	Streptococcal group	Source
S. pneumoniae R6	Yes	Mitis	J.P. Claverys
S. pneumoniae D39	Yes	Mitis	(22)
S. mitis SK142	Yes	Mitis	M. Kilian
S. oralis ATCC10557	Yes	Mitis	M. Kilian
S. peroris SK958	Yes	Mitis	M. Kilian
S. infantis SK140	Yes	Mitis	M. Kilian
S. sanguinis SK90	Yes	Mitis	M. Kilian
S. parasanguinis ATCC15912	Yes	Mitis	M. Kilian
S. gordonii SK6	Yes	Mitis	M. Kilian
S. cristatus NCTC12479	Yes	Mitis	M. Kilian
S. vestibularis NCTC 12166	Yes	Salivarius	M. Kilian
S. bovis NCTC8177	Yes	Bovis	M. Kilian
S. agalactiae NCTC8181	No	Pyogenes	M. Kilian
S. phocae ATCC29128	Yes	Pyogenes	M. Kilian
S. criceti ATCC19642	Yes	Mutans	M. Kilian
S. mutans NCTC10449	Yes	Mutans	M. Kilian
S. anginosus SK87	Yes	Anginosus	M. Kilian
B. subtilis ATCC6051	Moderate		ATCC
M. smegmatis NCTC8159	No		UKHSA
E. coli DH5a	No		Invitrogen
Pseudomonas brenneri	No		Lab stock, This study
L. lactis MG1363	No		Lab stock
S. aureus NCTC8325	No		Lab stock
E. faecalis LMG2708	No		Lab stock

Inactivation of the Ami oligopeptide transporter renders *S. pneumoniae* immune against lysinicin OF.

Our results suggested that lysinicin OF could be an antimicrobial peptide with characteristics similar to bacteriocins. Bacteriocins of Gram-positive bacteria typically recognise specific receptor molecules on the surface of their target bacteria. Once bound to the receptor the bacteriocins form a lethal pore in the cell membrane, either by themselves or in complex with the receptor (23-30). To identify a potential receptor of lysinicin OF, we checked if *S. pneumoniae* could develop resistance to the compound. As described above, a soft-agar overlay

containing *S. pneumoniae* resulted in a large inhibition zone surrounding the spotted colony of *Lysinibacillus* sp. OF-1 (Fig. 1A). The plate was incubated at 37°C for a prolonged period of time and already after 48 hours, we observed several colonies within the inhibition zone (Fig. 1A). Four of them were picked and re-streaked on TH-agar to make pure cultures. After identifying them as *S. pneumoniae* by 16S rRNA sequencing, their tolerance to lysinicin OF were tested in both soft-agar overlays and in liquid cultures (Fig. 2 and Fig. S4B). In these experiments all four isolates showed full immunity against lysinicin OF, even when grown with a concentration 10 times higher than the relative MIC determined for lysinicin OF (Fig. S5). The resistant mutants were named mutant1, -2, -3 and -4. The lysinicin OF resistance, however, appeared to come with a fitness cost, since all four mutants displayed reduced growth compared to the parental wildtype strain (Fig. 2). To identify these mutations, we sequenced the whole genome of mutant 1-4 and mapped the reads to the R6 reference genome (NC_003098.1). Strikingly, all had mutations in the *ami* operon (Table 2 and Fig. 2A). The *amiACDEF* genes code for an oligopeptide uptake system of the ATP-binding cassette (ABC) transporter type (31, 32). In *S. pneumoniae* this system has been shown to transport peptides of 2-7 amino acids, however, longer peptides have not been tested for this species (33). The Ami-system in *S. thermophilus*, on the other hand, has been shown to internalize peptides of up to 23 amino acids (34).

In the Ami-system, the lipoprotein AmiA binds extracellular peptides and pass them on to a peptide translocation channel composed of the two non-homologous membrane proteins, AmiC and AmiD. Peptides bound to AmiCD are then internalized most probably because the AmiCD channel undergoes a conformational change powered by ATP hydrolysis by the two associated cytoplasmic ATPases AmiE and AmiF (31). Mutant1, -2 and -4 had a point mutation in *amiC*, *amiE* and *amiF*, respectively, that resulted in premature termination of mRNA translation (stop codon in codon 223, 318 and 36, respectively). Mutant 3 had a deletion that

339 removed the end of *amiE* and the beginning of *amiF* (the DNA sequence coding for the last
340 147 amino acids of AmiE and first 161 amino acids of amiF was deleted). All four mutations
341 thus most probably resulted in an inactive Ami-system, which no longer can import
342 extracellular peptides.

343 To confirm that inactivation of the Ami-system results in resistance to lysinicin OF, we
344 used the sensitive RH425 strain and created a Δ*amiC* and a Δ*amiEF* mutant and treated them
345 with lysinicin OF. Similar to mutant1-4, inactivation of the Ami-system (Δ*amiC* and Δ*amiEF*)
346 resulted in full immunity against lysinicin OF and reduced growth (Fig. 2 and Fig. S4B).
347 Reduced growth of Ami-mutants has also been previously reported by Alloing and co-workers
348 (31). Microscopic examination of the Δ*amiC* mutant revealed severe morphological
349 abnormalities (Fig. 2D), corroborating the fitness cost that comes with lysinicin OF resistance.

350 Table 2. Mutations found in lysinicin OF resistant *S. pneumoniae* mutants.

Mutant nr.	Mutation type	Position on ref. genome (NC_003098.1)	Affected gene(s)	Consequence
1	SNP, C→T	1676261	*amiC*	Stop codon
2	SNP, G→A	1673543	*amiE*	Stop codon
3	Deletion	Δ1672934- 1674011	*amiEF*	Disrupted AmiE and AmiF
4	SNP, G→T	1673313	*amiF*	Stop codon

351

352

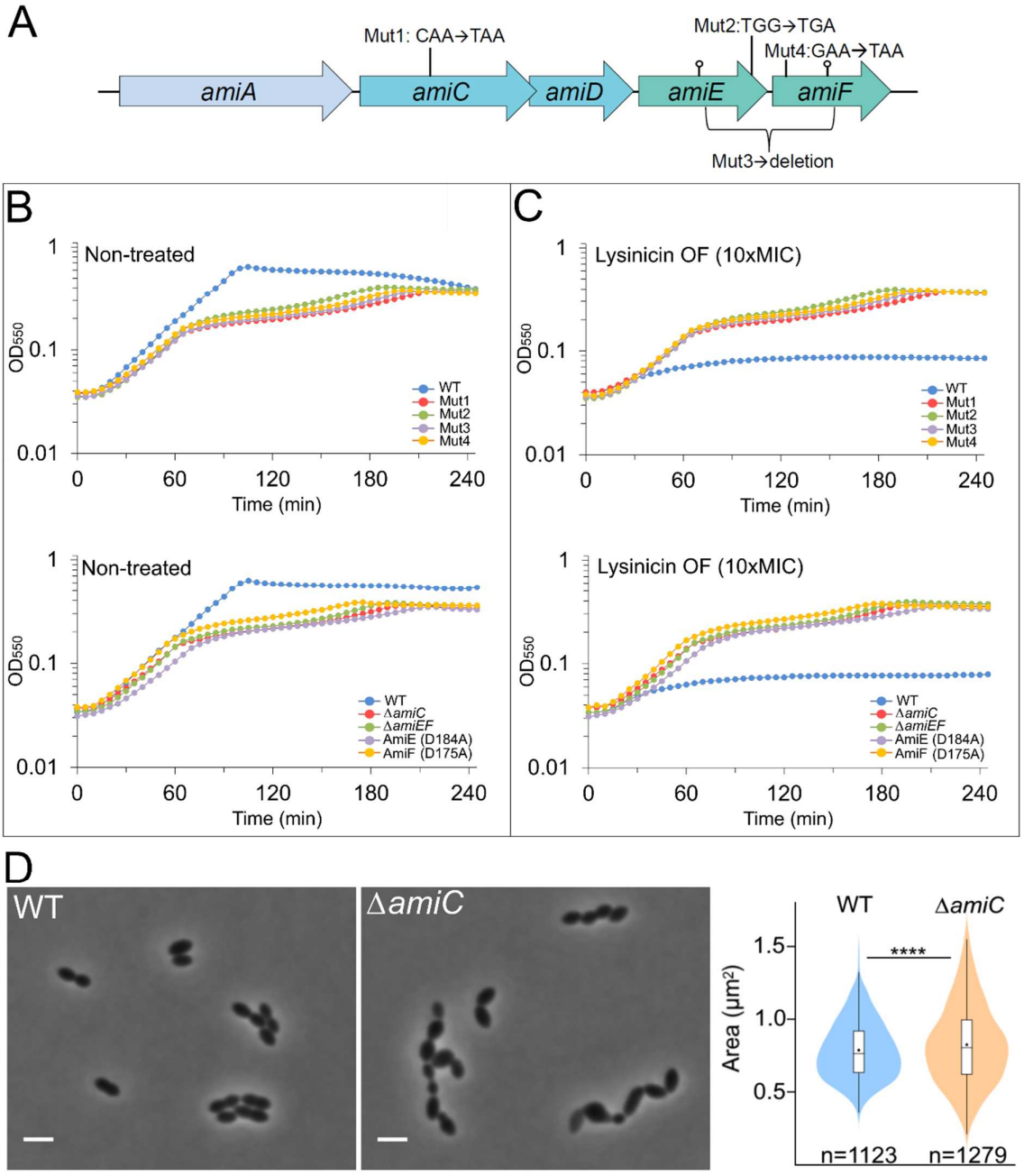

Fig. 2. Lysinicin OF sensitivity of *S. pneumoniae ami* mutants. (A) Schematic diagram of the *ami* operon depicting the mutations in mutant 1-4 (see Table 2) and codon position of D184 and D175 in *amiE* and *amiF* (lollipops). Mutant 1-4, Δ*amiC*, Δ*amiEF*, $amiE^{D184A}$, $amiF^{D175A}$ and wild type cells (strain RH425) were grown without (B) or in the presence (C) of 10 µl/ml lysinicin OF (10xMIC). All mutants expressing a compromised Ami-system displayed resistance towards lysinicin OF, whereas the growth of wild type was significantly inhibited. (D) The lysinicin OF resistant Δ*amiC* mutant displayed cells of heterogenous sizes with an average size of 0.83 ± 0.27 µm^2 compared with 0.79 ± 0.20 µm^2 for wild type. P-value were obtained relative to wild type using one-way Anova analysis, ****P<0.0001. Scale bars are 2 µm.

The bactericidal effect of lysinicin OF depends on ATP hydrolysis by the Ami-system.

Resistance to lysinicin OF was obtained by disruption of the Ami-system. This suggests that the Ami-system functions as a lysinicin OF receptor to facilitate pore formation in the cell membrane, or alternatively, that lysinicin OF is taken up via the Ami-system to execute its lethal action inside the cell. Translocation of extracellular peptides across the membrane depends on the ATPases AmiE and AmiF, which consume ATP to induce a conformational change in the AmiCD permease (31, 35). To test which of the abovementioned hypotheses that is true, we created two mutants in which the Ami-systems were kept intact except for their ability to hydrolyse ATP. We reasoned that if such mutants were still sensitive, lysinicin OF most likely use the Ami-system as a membrane embedded receptor. On the other hand, if these mutants became resistant to lysinicin OF, it supported the idea that lysinicin OF must enter the cell/cytoplasm to become lethal. Both AmiE and AmiF have the typical Walker A (GxxxxGKS/T where x can be various amino acids) and Walker B (hhhhD(D/E) where h is hydrophobic amino acids) motifs found in ATPases (Fig. S6). Walker A primarily binds ATP, while Walker B executes the ATP hydrolysis (36-38). The Walker B motif contains a conserved aspartic acid residue, which coordinates a Mg^{2+}-ion essential for ATP hydrolysis (38). Substitution of this aspartic acid residue with alanine in homologous ATPases has been shown to inactivate their ATPase activity (39, 40). By aligning the amino acid sequences of AmiE and AmiF against a homologous ATPase (DppD) from *Caldanaerobacter subterraneus* sp. *tengcongensis* for which the 3D-structure in complex with ATP and Mg^{2+} has been solved (Fig. S6), Asp184 were identified in AmiE and Asp175 in AmiF. We created two mutants in which one had replaced the native AmiE with the AmiE(D184A) version and in the other AmiF was replaced with AmiF(D175A). Similar to all the other lysinicin OF resistant mutants, they grew slower than wild type cells in addition to being resistant to lysinicin OF (Fig. 2 and Fig. S4). This showed that an intact, but inactive Ami-system makes *S. pneumoniae* resistant to lysinicin

389 OF, supporting that the compound is taken up by the cells. Worth noting, this phenotype could
390 not be attributed to destabilisation of the mutated AmiEF proteins since immunoblotting
391 showed that the expression levels of the mutated variants were comparable with wild type
392 AmiEFs (Fig. S7).

393 To further understand how the Ami-system affects lysinicin OF activity, we exposed a
394 Δ*amiA* mutant to lysinicin OF (AmiA binds extracellular peptides and provide them to the
395 AmiCDEF complex for import) (31, 33). Unexpectedly, AmiA deficient cells displayed similar
396 sensitivity to lysinicin OF as wild type cell (Fig. S8). Contrary to our previous result, this
397 indicated that lysinicin OF is not imported into the cytoplasm to kill the target cells, although
398 an ATP consuming Ami-system is a prerequisite for its activity. To exclude the possibility of
399 redundancy by the AmiA paralogs AliA and AliB (33), we tested lysinicin OF susceptibility of
400 a Δ*amiA*, Δ*aliA*, Δ*aliB* triple mutant. Similar to wild type, this mutant was also sensitive (Fig.
401 S8). Together, this shows that the activity of lysinicin OF depends on an intact AmiCD
402 permease and active ATP hydrolysis by AmiEF, however, the peptide binding protein AmiA
403 is not involved in the mechanism of action.

404

405 **Lysinicin OF does not disturb the cell membrane integrity.**

406 One of our hypotheses was that lysinicin OF uses the AmiCDEF complex as a docking
407 molecule in order to interfere with the cytoplasmic membrane of target cells. We did observe
408 that the toxic effect of lysinicin OF was nearly irreversible, i.e., inhibiting cell growth without
409 the possibility of recovering after lysinicin OF removal (Fig. S9). This is compatible with a
410 model where lysinicin OF induces a biophysical change in the cells, e.g. interfering with the
411 membrane integrity. To further test this hypothesis, we determined if the membrane of lysinicin
412 OF treated cells became permeable to the fluorescent dye Sytox Green. This fluorophore

fluoresces upon binding DNA, however, it is not able to cross intact cell membranes. Hence, disintegration of the cell membrane can be detected as increased fluorescence. *S. pneumoniae* RH425 were grown in the presence of 2 µM Sytox® Green. At OD_{550} = 0.25, lysinicin OF was added to a final concentration of 10 times the relative MIC value. Nisin was used as a control (see Fig. S5 for MIC values) representing a pore forming peptide (41-43) and Triton X-100 as a membrane dissolving detergent. After addition of lysinicin OF, the cell growth levelled out within an hour, but no increase in fluorescence was detected (Fig 3A). Nisin and Triton X-100, on the other hand, resulted in reduced cell densities and a significant increase in fluorescence, showing that also pneumococcal autolysis is induced when the membrane integrity is disrupted. Similarly, dead/live staining and fluorescence microscopy showed that the cytoplasmic membrane is intact after exposure to 10 x MIC of lysinicin OF for 30 minutes (Fig. 3B). The pore forming peptide nisin on the other hand clearly permeabilized the cytoplasmic membrane. Since no membrane destabilizing effect was detected for *S. pneumoniae* upon lysinicin OF treatment, we checked whether eukaryotic cell membranes also could tolerate this compound. A common obstacle of many new antimicrobials is that they disrupt eukaryotic cell membranes causing hemolysis (44, 45). In the case of lysinicin OF, however, treatment of sheep blood cells with 10xMIC of lysinicin OF did not lead to hemolysis (Fig. S10).

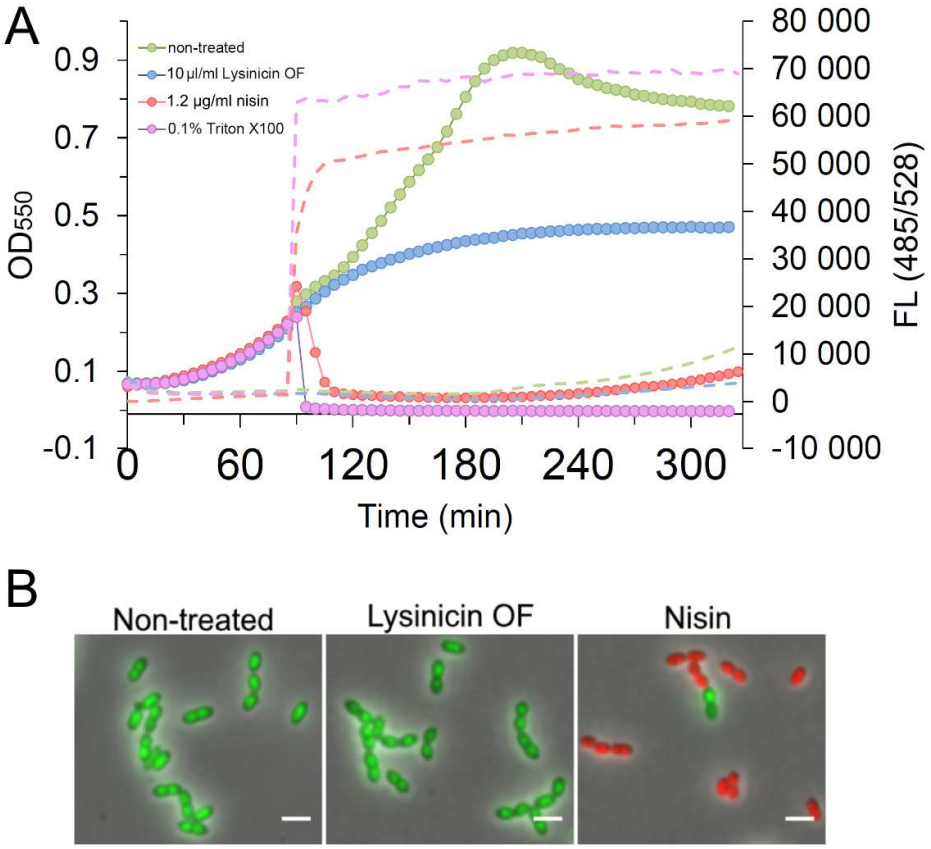

Fig. 3. The effect of lysinicin OF on cell membrane integrity. (A) *S. pneumoniae* was grown in the presence of the nucleic acid stain Sytox® Green, which fluoresces upon DNA binding when excited at 485 nm. Since Sytox® Green is unable to cross intact cell membranes, an increase in fluorescent signal is directly correlated with reduced cell membrane integrity. At OD_{550} = 0.25 lysinicin OF was added to a final concentration of 10xMIC. The optical density (circles) and fluorescent signal (dotted lines) were recorded every fifth minute. The pore forming peptide nisin (10xMIC) and the detergent Triton X-100 (0.1%, v/v) were used as known membrane interfering controls. (B) Dead/live staining of *S. pneumoniae* (Δ*lytA*) treated with 10xMIC lysinicin OF or nisin for 30 minutes. Cells with intact cytoplasmic membranes appear green, while cells having a leaky cell membrane are red. Scale bars are 2 µm.

Morphology of lysinicin OF treated pneumococci.

Antibiotics inhibiting cell wall synthesis or DNA replication often induce characteristic changes to bacterial cell size and/or shapes and nucleoid topology, respectively (46-49). To obtain clues to lysinicin OF's mode of action, morphological characteristics of lysinicin OF treated cells (1xMIC) were compared to cells treated with a selection of antibiotics (1xMIC)

targeting cell wall synthesis (ampicillin), DNA replication (ciprofloxacin), transcription (rifampicin) and protein synthesis (tetracycline) (50-57). The nucleoids were also examined by DAPI staining and fluorescence microscopy. Phase contrast imaging did not reveal any dramatic changes to the cell morphology of lysinicin OF treated cells. However, using the microbeJ analysis tool (12), a reduction in average cell size was observed (from 0.79 ± 0.20 μm^2 to 0.67 ± 0.18 μm^2) (Fig. 4A). The cell size was not further reduced by increasing the lysinicin OF concentration to 10x MIC (Fig. S11). Furthermore, lysinicin OF treatment did not cause formation of anucleate cells, but the DAPI signals became clearly more concentrated (Fig. 4B). This suggests that DNA was more condensely packed in cells inhibited by lysinicin OF. None of the other antibiotics produced cells with exact similar characteristics as lysinicin OF treatment. For example, ampicillin treatment resulted in major morphological abnormalities (bloated and elongated cells), while neither rifampicin nor tetracycline resulted in significant cell morphology or cell size changes. We did see a small reduction in average cell size and concentrated DAPI signals for ciprofloxacin. However, ciprofloxacin also produced several anucleated cells, which were not the case for lysinicin OF. Rifampicin were also found to produce some anucleated cells, in line with what has been reported previously in pneumococci (58) (rifampicin is also known to inhibit initiation of replication (59)). Concentrated DAPI signals were observed for tetracyclin, but no reduction in cell size. Taken together, none of the antibiotics tested induced cellular changes identical to lysinicin OF, although similar nucleoid topology as for the translation inhibitor tetracycline was seen.

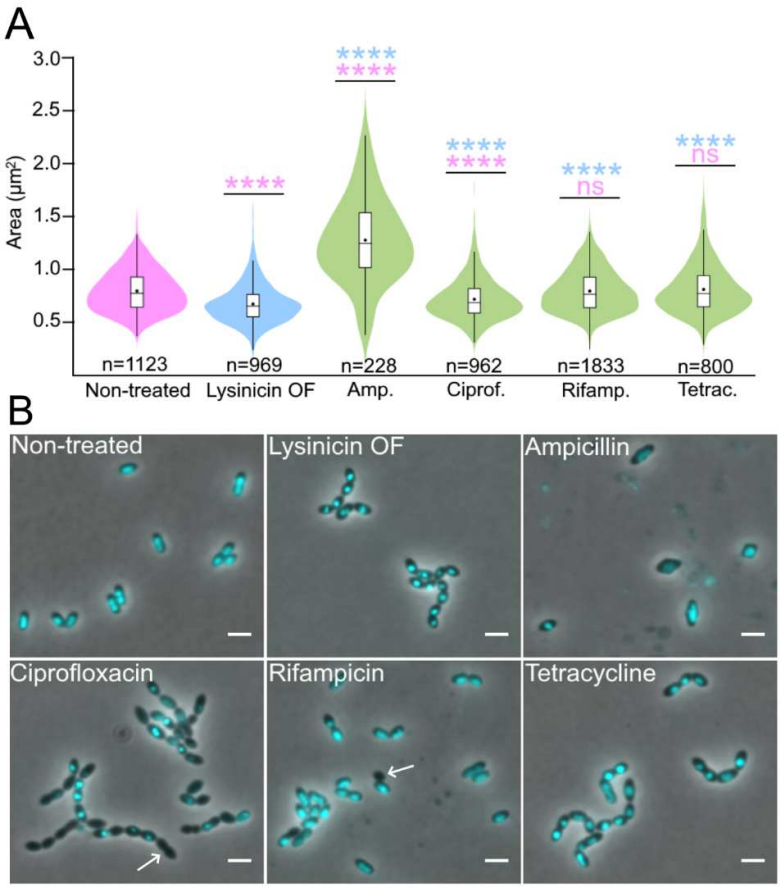

468

469 **Fig. 4.** Comparison of the morphology and chromosome distribution in *S. pneumoniae* RH425
470 treated with lysinicin OF and different antibiotics. A. Violin plot of the average cell size (μm^2)
471 after treatment with 1xMIC of the indicated antimicrobials (see Fig. S5) for four hours at 37°C.
472 The antibiotics were added at OD = 0.1. Compared to non-treated cells (0.79 ± 0.20 μm^2),
473 ampicillin (1.27 ± 0.40 μm^2) and ciprofloxacin (0.71 ± 0.19 μm^2) treatment changed the
474 average cell size, whereas rifampicin (0.79 ± 0.20 μm^2) and tetracycline (0.80 ± 0.23 μm^2) did
475 not. Lysinicin OF treatment resulted in smaller cells (0.67 ± 0.18 μm^2) compared to any other
476 treatment. P values were obtained relative to non-treated cells (pink) or lysinicin OF treated
477 cells (blue) using one-way analysis of variance (ANOVA). ****, $P < 0.00001$. B. The cells
478 were incubated with antibiotics as described for panel A. DNA was labelled with DAPI and
479 cells were imaged by phase contrast and fluorescence microscopy. Arrows indicate anucleated
480 cells. Scale bars are 2 µm.

481

482 **Discussion.**

483 In a screen for anti-pneumococcal compounds among marine bacteria sampled from the Oslo
484 Fjord (Norway), one isolate stood out with strong inhibitory effect. Whole genome sequencing
485 (accession number in GeneBank, CP102798) placed it in the genus *Lysinibacillus* sharing

sequence similarities with the species *L. sphaericus* and *L. fusiformis*. The isolate, named *Lysinibacillus* sp. OF-1, produces an anti-pneumococcal compound of proteinaceous nature that we named lysinicin OF. A few previous studies have reported that members of the *Lysinibacillus* genus produce antimicrobials of proteinaceous nature such as heat labile bacteriocins (inactivated >80°C) and lipopeptides (60-62). Since lysinicin OF could resist both heat (100°C) and polymyxin acylase treatment (cleaves off the peptide part of lipopeptides), we concluded that it most probably is a peptide. Furthermore, BAGEL4 and AntiSMASH mining did not find any gene clusters of known antimicrobials in the *Lysinibacillus* sp. OF-1 genome, suggesting that lysinicin OF is a new antimicrobial peptide. Attempts to identify its mass and amino acid sequence by combining reverse phase UHPLC and MALDI-TOF MS-MS have unfortunately not succeeded, and we therefore do not know the exact nature of this compound. The explanation for this is that we were unable to obtain a sample of sufficient purity. It is possible that the hydrophobic characteristics of lysinicin OF (binds XAD Amberlite and C18) make it stick to other hydrophobic components in growth medium supernatants that are not removed by the C18 reverse phase chromatography and acetonitrile gradient elution used here. It would be worth exploring other eluents and solid phases as well as solvent extraction techniques to produce a sample compatible with mass identification and NMR analysis. Clues about its structure could also be obtained by inactivating genes involved in the biosynthesis of this molecule, e.g., by creating a transposon library of the *Lysinibacillus* sp. OF-1 isolate.

We discovered that lysinicin OF employs the oligo peptide permease Ami in target cells to execute its lethal action. The observation that molecules inhibit growth of *S. pneumoniae* by exploiting the Ami-system is not new. In fact, specific peptides derived from ribosomal proteins of Gammaproteobacteria and folate analogues (methotrexate and aminopterin) have been shown to use the Ami-system for preventing pneumococcal growth (63, 64). The exact

511 mechanisms of these peptides and folate analogues, however, remain unknown. Although these
512 oligo peptide permeases are widespread among bacteria (65), lysinicin OF has a narrow target
513 range limited to streptococcal species (except for *S. agalactiae* NCTC8181) and to some extent
514 to *B. subtilis*. The Gram negatives *P. brenneri* and *E. coli* as well as the Gram positives *M.*
515 *smegmatis*, *L. lactis*, *S. aureus* and *E. faecalis* were resistant. Using the pneumococcal AmiC
516 as reference of a lysinicin OF sensitive Ami-system, sequence comparison of the AmiC
517 homologous in these species with the pneumococcal AmiC (Table S3) showed that a sequence
518 identity lower than 34% conferred natural tolerance to lysinicin OF. However, there are
519 exceptions, e.g *S. bovis* NCTC8177 (26%), *S. criceti* ATCC19642 (27%) and *S. mutans*
520 NCTC10449 (28%). Although having lower homology with AmiC than for example the *E. coli*
521 homologue DppB (34%), these Ami-systems probably still have specific structural features and
522 sequence motifs found in pneumococcal Ami, making them recognizable to lysinicin OF.

523 We showed that cells expressing an intact but inactive Ami-system, i.e., Walker B
524 mutated AmiE or AmiF became completely resistant to lysinicin OF. Combined with the sytox
525 assay and dead/live staining, which showed that lysinicin OF did not interfere with cell
526 membrane integrity, it is plausible that the compound is taken up through the Ami-system to
527 hit a cytoplasmic target. If lysinicin OF indeed is a peptide, one would expect that it uses the
528 Ami-system for internalization and cells thus become resistant when the Ami-system is unable
529 to import peptides. If so, why was a Δ*amiA*, Δ*aliA*, Δ*aliB* triple mutant still sensitive? The Ami-
530 system uses either of these lipoproteins to shuttle peptides through the AmiCD channel, and a
531 triple mutant has been shown to have equal oligopeptide transport deficiency as mutants
532 lacking AmiCDE or F (33). Two alternative explanations are possible: (i) lysinicin OF is not
533 taken up by the Ami-system, but instead binds the active form of AmiCDEF to induce a
534 conformational change in the complex, e.g. affecting the transmembrane electric potential. It
535 is known that the folic acid derivates aminopterin and methotrexate, which have been used as

antineoplastic drugs, inhibit growth of wild type *S. pneumoniae*, but not in Ami deficient mutants (63, 66). Methotrexate was shown to increase the transmembrane electric potential when Ami was intact, but the exact mechanism is unknown (63). The smallest membrane pores detectable by the sytox assay must allow molecules larger than 278 Da to cross the membrane (MW of Sytox green is 278.329 Da), whereas changes in the transmembrane electric potential would only require opening of an ion-channel (67). A reasonable question is whether lysinicin OF could freeze the AmiCD complex in an open conformation allowing ions to freely cross the cell membrane. (ii) Alternatively, lysinicin OF can by-pass the requirement of AmiA, AliA and AliB and cross the membrane through the AmiCD channel in its open conformation (AmiEF must be active).

Neither ciprofloxacin, ampicillin, rifampicin, or tetracycline induced phenotypic changes identical to lysinicin OF in *S. pneumoniae*, i.e., reduced cell size and condensed DNA (Fig. 4). Although DNA condensation was also seen for both ciprofloxacin and tetracycline, ciprofloxacin produced several anucleated cells, while tetracycline treatment did not significantly reduce the average cell size. Based on the phenotypic comparison it seems unlikely that lysinicin OF inhibits cell wall synthesis (ampicillin) or transcription (rifampicin), but that its toxic effect somehow could interfere with DNA- or protein synthesis. A group of small (<5 kDa) post translationally modified peptides called class I microcins are known to kill bacteria by inhibiting RNA-, DNA- and protein synthesis (68). However, these are produced by enterobacteria (primarily by *E. coli*). Microcin-like peptides are yet to be found produced by Gram-positive bacteria. Whether lysinicin OF is internalized by sensitive cells similar to class I microcins, or if it acts on the outside somehow transforming the Ami-system into a lethal weapon is still unclear at the moment.

Combined with its quick and almost irreversible lethal effect, lysinicin OF could be an interesting molecule to explore for possible therapeutic applications., e.g. prevention of

561 streptococcal host colonization that can lead to skin, soft-tissue, and mammary glands
562 infections or within preventative dentistry as an anti-biofilm molecule (mutans group) (69).
563 However, this study has shown that the antimicrobial potential of lysinicin OF has challenges
564 in terms of resistance development. Full resistance was obtained by inactivation of the Ami
565 system, and Ami deficient mutants would likely emerge when exposed to lysinicin OF. It has
566 been shown for *S. pneumoniae* that Ami is important for colonization of the host, but not during
567 invasive infection (70). Therefore, lysinincin OF could have higher potential to prevent
568 streptococcal host colonization rather than for treatment strategies. To further elucidate its
569 therapeutic potential, future investigations should focus on solving the structure and mode of
570 action of this molecule.

571

572 **Acknowledgements.**

573 We thank Dr. Thomas A. H. Haverkamp at the Norwegian Veterinary Institute for help
574 processing the long read DNA sequencing data. We also thank Maria Disen Barbuti at the
575 Norwegian University of Life Sciences for valuable technical assistance, testing lysinicin OF
576 in different experimental setups.

577

578 **Funding information.**

579 This study was funded by the Research Council of Norway, project number 287416.

580

581 **Data summary.**

582 The genome sequence of *Lysinibacillus* sp. OF-1 is accessible in GenBank under the accession
583 number CP102798.

Author contributions.

DS, LSH and MK designed the study. IHH, VS, DS, ZS and ARW performed the experiments. CAB sequenced and assembled bacterial genomes in the present study. DS, LSH, MK, IHH and VS analysed the data. DS, MK, LSH and CAB wrote the manuscript.

Conflicts of interest.

All authors declare no conflicts of interest.

References.

1. IACG. NO TIME TO WAIT: SECURING THE FUTURE FROM DRUG-RESISTANT INFECTIONS. 2019.
2. WHO. Global Antimicrobial Resistance Surveillance System (GLASS) Report Early implementation. 2017.
3. O'Brien KL, Wolfson LJ, Watt JP, Henkle E, Deloria-Knoll M, McCall N, et al. Burden of disease caused by *Streptococcus pneumoniae* in children younger than 5 years: global estimates. Lancet. 2009;374(9693):893-902.
4. Cherazard R, Epstein M, Doan TL, Salim T, Bharti S, Smith MA. Antimicrobial Resistant *Streptococcus pneumoniae*: Prevalence, Mechanisms, and Clinical Implications. Am J Ther. 2017;24(3):e361-e9.
5. Chewapreecha C, Harris SR, Croucher NJ, Turner C, Marttinen P, Cheng L, et al. Dense genomic sampling identifies highways of pneumococcal recombination. Nat Genet. 2014;46(3):305-9.
6. Aminov RI. A brief history of the antibiotic era: lessons learned and challenges for the future. Front Microbiol. 2010;1:134.
7. Newman DJ, Cragg GM. Natural products as sources of new drugs over the last 25 years. J Nat Prod. 2007;70(3):461-77.
8. Lacks S, Hotchkiss RD. A study of the genetic material determining an enzyme activity in pneumococcus. Biochimica et biophysica acta. 1960;39(3):508-18.
9. Higuchi R, Krummel B, Saiki RK. A general method of in vitro preparation and specific mutagenesis of DNA fragments: study of protein and DNA interactions. Nucleic Acids Res. 1988;16(15):7351-67.
10. Sung C, Li H, Claverys J, Morrison D. An *rpsL* cassette, janus, for gene replacement through negative selection in *Streptococcus pneumoniae*. Applied and environmental microbiology. 2001;67(11):5190-6.
11. Seemann T. Prokka: rapid prokaryotic genome annotation. Bioinformatics. 2014;30(14):2068-9.
12. Ducret A, Quardokus EM, Brun YV. MicrobeJ, a tool for high throughput bacterial cell detection and quantitative analysis. Nat Microbiol. 2016;1(7):16077.
13. Laemmli UK. Cleavage of structural proteins during the assembly of the head of bacteriophage T4. Nature. 1970;227(5259):680-5.

14. Stamsås GA, Straume D, Salehian Z, Håvarstein LS. Evidence that pneumococcal WalK is regulated by StkP through protein-protein interaction. Microbiology (Reading, England). 2017;163(3):383-99.
15. Avram O, Rapoport D, Portugez S, Pupko T. M1CR0B1AL1Z3R-a user-friendly web server for the analysis of large-scale microbial genomics data. Nucleic Acids Res. 2019;47(W1):W88-W92.
16. van Heel AJ, de Jong A, Song C, Viel JH, Kok J, Kuipers OP. BAGEL4: a user-friendly web server to thoroughly mine RiPPs and bacteriocins. Nucleic Acids Res. 2018;46(W1):W278-W81.
17. Blin K, Shaw S, Kloosterman AM, Charlop-Powers Z, van Wezel GP, Medema MH, et al. antiSMASH 6.0: improving cluster detection and comparison capabilities. Nucleic Acids Res. 2021;49(W1):W29-W35.
18. Steller S, Vollenbroich D, Leenders F, Stein T, Conrad B, Hofemeister J, et al. Structural and functional organization of the fengycin synthetase multienzyme system from *Bacillus subtilis* b213 and A1/3. Chem Biol. 1999;6(1):31-41.
19. Abriouel H, Franz CM, Ben Omar N, Galvez A. Diversity and applications of *Bacillus* bacteriocins. FEMS Microbiol Rev. 2011;35(1):201-32.
20. Caulier S, Nannan C, Gillis A, Licciardi F, Bragard C, Mahillon J. Overview of the Antimicrobial Compounds Produced by Members of the Bacillus subtilis Group. Front Microbiol. 2019;10:302.
21. Yim G, Thaker MN, Koteva K, Wright G. Glycopeptide antibiotic biosynthesis. J Antibiot (Tokyo). 2014;67(1):31-41.
22. Slager J, Aprianto R, Veening JW. Deep genome annotation of the opportunistic human pathogen *Streptococcus pneumoniae* D39. Nucleic Acids Res. 2018;46(19):9971-89.
23. Diep DB, Skaugen M, Salehian Z, Holo H, Nes IF. Common mechanisms of target cell recognition and immunity for class II bacteriocins. Proc Natl Acad Sci U S A. 2007;104(7):2384-9.
24. Kjos M, Oppegard C, Diep DB, Nes IF, Veening JW, Nissen-Meyer J, et al. Sensitivity to the two-peptide bacteriocin lactococcin G is dependent on UppP, an enzyme involved in cell-wall synthesis. Mol Microbiol. 2014;92(6):1177-87.
25. Oftedal TF, Ovchinnikov KV, Hestad KA, Goldbeck O, Porcellato D, Narvhus J, et al. Ubericin K, a New Pore-Forming Bacteriocin Targeting mannose-PTS. Microbiol Spectr. 2021;9(2):e0029921.
26. Ovchinnikov KV, Kristiansen PE, Straume D, Jensen MS, Aleksandrzak-Piekarczyk T, Nes IF, et al. The Leaderless Bacteriocin Enterocin K1 Is Highly Potent against *Enterococcus faecium*: A Study on Structure, Target Spectrum and Receptor. Front Microbiol. 2017;8:774.
27. Zhu L, Zeng J, Wang C, Wang J. Structural basis of pore formation in the mannose phosphotransferase system (man-PTS) by pediocin PA-1. Appl Environ Microbiol. 2021:AEM0199221.
28. Perez-Ramos A, Madi-Moussa D, Coucheney F, Drider D. Current Knowledge of the Mode of Action and Immunity Mechanisms of LAB-Bacteriocins. Microorganisms. 2021;9(10).
29. Abee T, Klaenhammer TR, Letellier L. Kinetic studies of the action of lactacin F, a bacteriocin produced by *Lactobacillus johnsonii* that forms poration complexes in the cytoplasmic membrane. Appl Environ Microbiol. 1994;60(3):1006-13.
30. Hechard Y, Sahl HG. Mode of action of modified and unmodified bacteriocins from Gram-positive bacteria. Biochimie. 2002;84(5-6):545-57.
31. Alloing G, Trombe MC, Claverys JP. The *ami* locus of the gram-positive bacterium *Streptococcus pneumoniae* is similar to binding protein-dependent transport operons of gram-negative bacteria. Mol Microbiol. 1990;4(4):633-44.
32. Rees DC, Johnson E, Lewinson O. ABC transporters: the power to change. Nat Rev Mol Cell Biol. 2009;10(3):218-27.
33. Alloing G, de Philip P, Claverys JP. Three highly homologous membrane-bound lipoproteins participate in oligopeptide transport by the Ami system of the gram-positive *Streptococcus pneumoniae*. J Mol Biol. 1994;241(1):44-58.
34. Garault P, Le Bars D, Besset C, Monnet V. Three oligopeptide-binding proteins are involved in the oligopeptide transport of *Streptococcus thermophilus*. J Biol Chem. 2002;277(1):32-9.
35. Davidson AL. Mechanism of coupling of transport to hydrolysis in bacterial ATP-binding cassette transporters. J Bacteriol. 2002;184(5):1225-33.

36. Khan YA, White KI, Brunger AT. The AAA+ superfamily: a review of the structural and mechanistic principles of these molecular machines. Crit Rev Biochem Mol Biol. 2021:1-32.
37. Walker JE, Saraste M, Runswick MJ, Gay NJ. Distantly related sequences in the alpha- and beta-subunits of ATP synthase, myosin, kinases and other ATP-requiring enzymes and a common nucleotide binding fold. EMBO J. 1982;1(8):945-51.
38. Story RM, Steitz TA. Structure of the RecA protein-ADP complex. Nature. 1992;355(6358):374-6.
39. Sham LT, Jensen KR, Bruce KE, Winkler ME. Involvement of FtsE ATPase and FtsX extracellular loops 1 and 2 in FtsEX-PcsB complex function in cell division of *Streptococcus pneumoniae* D39. mBio. 2013;4(4).
40. Arends SJ, Kustusch RJ, Weiss DS. ATP-binding site lesions in FtsE impair cell division. J Bacteriol. 2009;191(12):3772-84.
41. Breukink E, Wiedemann I, van Kraaij C, Kuipers OP, Sahl HG, de Kruijff B. Use of the cell wall precursor lipid II by a pore-forming peptide antibiotic. Science. 1999;286(5448):2361-4.
42. Ruhr E, Sahl HG. Mode of action of the peptide antibiotic nisin and influence on the membrane potential of whole cells and on cytoplasmic and artificial membrane vesicles. Antimicrob Agents Chemother. 1985;27(5):841-5.
43. Wiedemann I, Breukink E, van Kraaij C, Kuipers OP, Bierbaum G, de Kruijff B, et al. Specific binding of nisin to the peptidoglycan precursor lipid II combines pore formation and inhibition of cell wall biosynthesis for potent antibiotic activity. J Biol Chem. 2001;276(3):1772-9.
44. Schmitt MA, Weisblum B, Gellman SH. Interplay among folding, sequence, and lipophilicity in the antibacterial and hemolytic activities of alpha/beta-peptides. J Am Chem Soc. 2007;129(2):417-28.
45. Wang G, Li X, Wang Z. APD3: the antimicrobial peptide database as a tool for research and education. Nucleic Acids Res. 2016;44(D1):D1087-93.
46. Lorian V, Atkinson B. Abnormal forms of bacteria produced by antibiotics. Am J Clin Pathol. 1975;64(5):678-88.
47. Georgopapadakou NH, Bertasso A. Effects of quinolones on nucleoid segregation in *Escherichia coli*. Antimicrob Agents Chemother. 1991;35(12):2645-8.
48. Rajendram M, Hurley KA, Foss MH, Thornton KM, Moore JT, Shaw JT, et al. Gyramides prevent bacterial growth by inhibiting DNA gyrase and altering chromosome topology. ACS Chem Biol. 2014;9(6):1312-9.
49. Hawkey PM. Mechanisms of quinolone action and microbial response. J Antimicrob Chemother. 2003;51 Suppl 1:29-35.
50. Hartmann G, Honikel KO, Knusel F, Nuesch J. The specific inhibition of the DNA-directed RNA synthesis by rifamycin. Biochim Biophys Acta. 1967;145(3):843-4.
51. Wehrli W, Knusel F, Schmid K, Staehelin M. Interaction of rifamycin with bacterial RNA polymerase. Proc Natl Acad Sci U S A. 1968;61(2):667-73.
52. Connamacher RH, Mandel HG. Binding of Tetracycline to the 30s Ribosomes and to Polyuridylic Acid. Biochem Biophys Res Commun. 1965;20:98-103.
53. Gale EF, Folkes JP. The assimilation of amino-acids by bacteria. XV. Actions of antibiotics on nucleic acid and protein synthesis in *Staphylococcus aureus*. Biochem J. 1953;53(3):493-8.
54. Izaki K, Matsuhashi M, Strominger JL. Glycopeptide transpeptidase and D-alanine carboxypeptidase: penicillin-sensitive enzymatic reactions. Proc Natl Acad Sci U S A. 1966;55(3):656-63.
55. Lawrence PJ, Strominger JL. Biosynthesis of the peptidoglycan of bacterial cell walls. XV. The binding of radioactive penicillin to the particulate enzyme preparation of *Bacillus subtilis* and its reversal with hydroxylamine or thiols. J Biol Chem. 1970;245(14):3653-9.
56. Sugino A, Peebles CL, Kreuzer KN, Cozzarelli NR. Mechanism of action of nalidixic acid: purification of *Escherichia coli nalA* gene product and its relationship to DNA gyrase and a novel nicking-closing enzyme. Proc Natl Acad Sci U S A. 1977;74(11):4767-71.
57. Emmerson AM, Jones AM. The quinolones: decades of development and use. J Antimicrob Chemother. 2003;51 Suppl 1:13-20.
58. Kjos M, Veening JW. Tracking of chromosome dynamics in live *Streptococcus pneumoniae* reveals that transcription promotes chromosome segregation. Mol Microbiol. 2014;91(6):1088-105.

59. von Meyenburg K, Hansen FG, Riise E, Bergmans HE, Meijer M, Messer W. Origin of replication, *oriC*, of the *Escherichia coli* K12 chromosome: genetic mapping and minichromosome replication. Cold Spring Harb Symp Quant Biol. 1979;43 Pt 1:121-8.
60. Ahmad V, Iqbal AN, Haseeb M, Khan MS. Antimicrobial potential of bacteriocin producing *Lysinibacillus* jx416856 against foodborne bacterial and fungal pathogens, isolated from fruits and vegetable waste. Anaerobe. 2014;27:87-95.
61. Akintayo SO, Treinen C, Vahidinasab M, Pfannstiel J, Bertsche U, Fadahunsi I, et al. Exploration of surfactin production by newly isolated *Bacillus* and *Lysinibacillus* strains from food-related sources. Lett Appl Microbiol. 2022;75(2):378-87.
62. Satapute P, Jogaiah S. A biogenic microbial biosurfactin that degrades difenoconazole fungicide with potential antimicrobial and oil displacement properties. Chemosphere. 2022;286(Pt 1):131694.
63. Trombe MC. Alteration of *Streptococcus pneumoniae* membrane properties by the folate analog methotrexate. J Bacteriol. 1984;160(3):849-53.
64. Nasher F, Aguilar F, Aebi S, Hermans PWM, Heller M, Hathaway LJ. Peptide Ligands of AmiA, AliA, and AliB Proteins Determine Pneumococcal Phenotype. Front Microbiol. 2018;9:3013.
65. Monnet V. Bacterial oligopeptide-binding proteins. Cell Mol Life Sci. 2003;60(10):2100-14.
66. Sicard AM. A New Synthetic Medium for *Diplococcus pneumoniae*, and Its Use for the Study of Reciprocal Transformations at the Amia Locus. Genetics. 1964;50:31-44.
67. Martinac B, Saimi Y, Kung C. Ion channels in microbes. Physiol Rev. 2008;88(4):1449-90.
68. Duquesne S, Destoumieux-Garzon D, Peduzzi J, Rebuffat S. Microcins, gene-encoded antibacterial peptides from enterobacteria. Nat Prod Rep. 2007;24(4):708-34.
69. Oda Y, Hayashi F, Okada M. Longitudinal study of dental caries incidence associated with *Streptococcus mutans* and *Streptococcus sobrinus* in patients with intellectual disabilities. BMC Oral Health. 2015;15:102.
70. Kerr AR, Adrian PV, Estevao S, de Groot R, Alloing G, Claverys JP, et al. The Ami-AliA/AliB permease of *Streptococcus pneumoniae* is involved in nasopharyngeal colonization but not in invasive disease. Infect Immun. 2004;72(7):3902-6.

Supplemental material for the article entitled: A novel proteinaceous molecule produced by *Lysinibacillus* sp. OF-1 depends on the Ami oligopeptide transporter to kill *Streptococcus pneumoniae*.

Ingvild Hals Hauge[1], Vilde Sandegren[1], Anja Ruud Winther[1], Cathrine Arnason Bøe[2], Zhian Salehian[1], Leiv Sigve Håvarstein[1], Morten Kjos[1] and Daniel Straume[1]*.

[1]Faculty of Chemistry, Biotechnology and Food Science, Norwegian University of Life Sciences, 1430 Ås, Norway.

[2]Norwegian Veterinary Institute, Department of Molecular Biology, 1433 Ås, Norway.

Fig. S1. Initial soft-agar overlay showing growth inhibition of *S. pneumoniae* RH425 by colonies isolated from a rock at the shore in the Oslo Fjord. The yellow arrows indicate colonies surrounded by smaller inhibition zones, while the white arrow indicates a colony identified as a *Lysinibacillus* species with strong inhibition of *S. pneumoniae*.

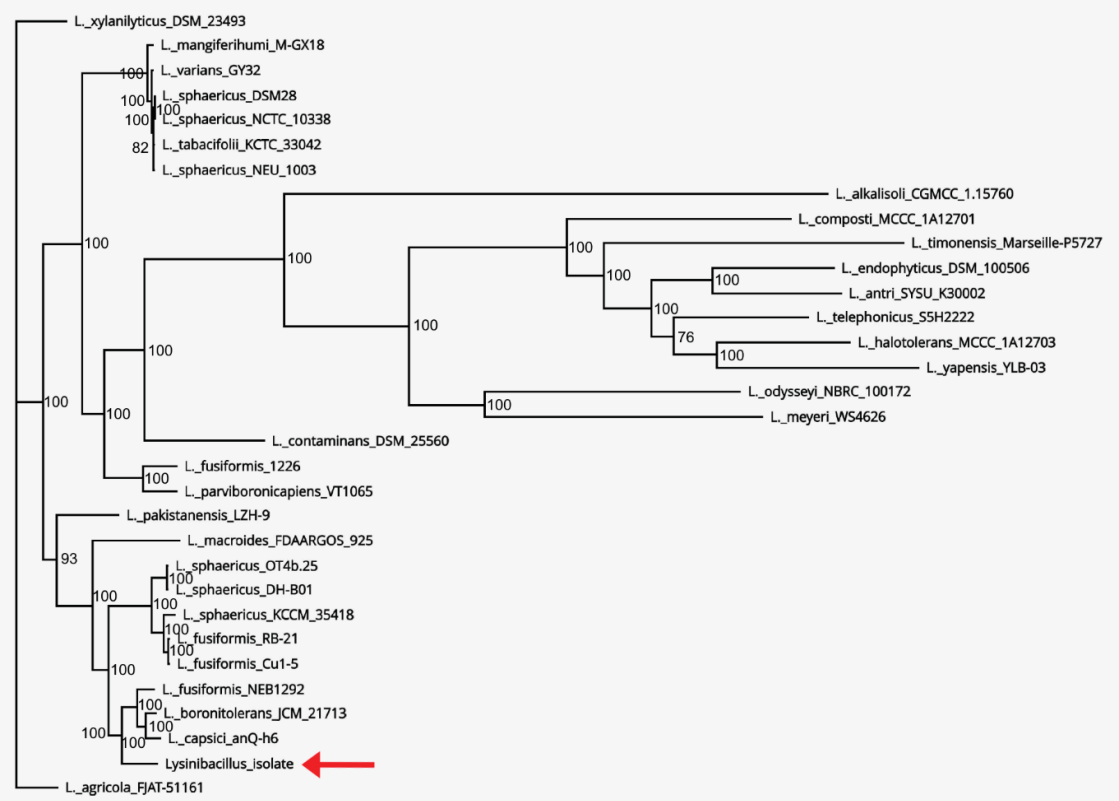

Fig. S2. Phylogram showing the evolutionary relationship of 31 lysinibacilli, including all 23 known species in this genus. *Lysinibacillus* sp. OF-1 is placed (red arrow) in a clade together with *L. fusiformis*, *L. boronitolerans* and *L. capsici*.

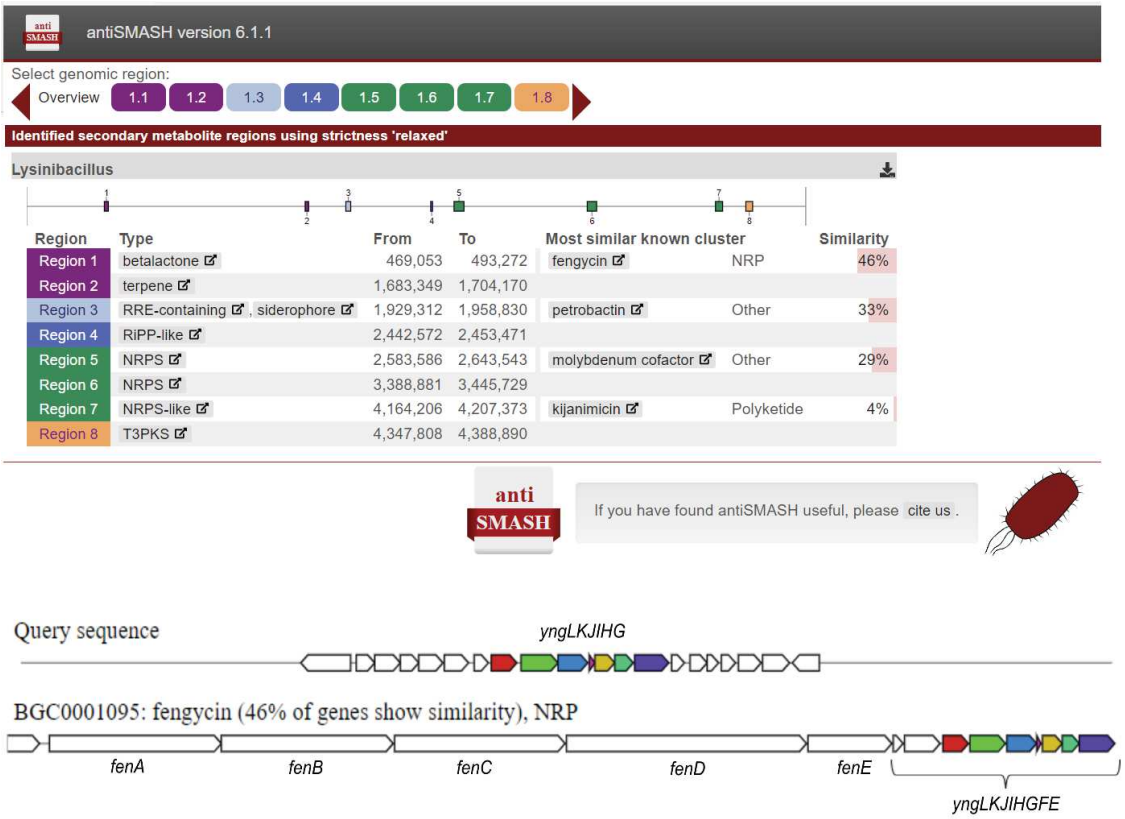

Fig. S3. antiSMASH output of the *Lysinibacillus* sp. OF-1 genome analysis. A 46% similarity (percentage of genes) to the fengycin biosynthesis cluster in *B. velezensis* FZB42 was found. The *Lysinibacillus* sp. OF-1 genome does not have the fengycin synthetase genes *fenABCDE* but has the *yngLKJIHG* genes, which are often found associated with fengycin synthetase genes (1). The exact functions of the *yng* genes are not known, but they have been suggested to be involved in lipid catabolism, leucine degradation and/or sporulation (2, 3).

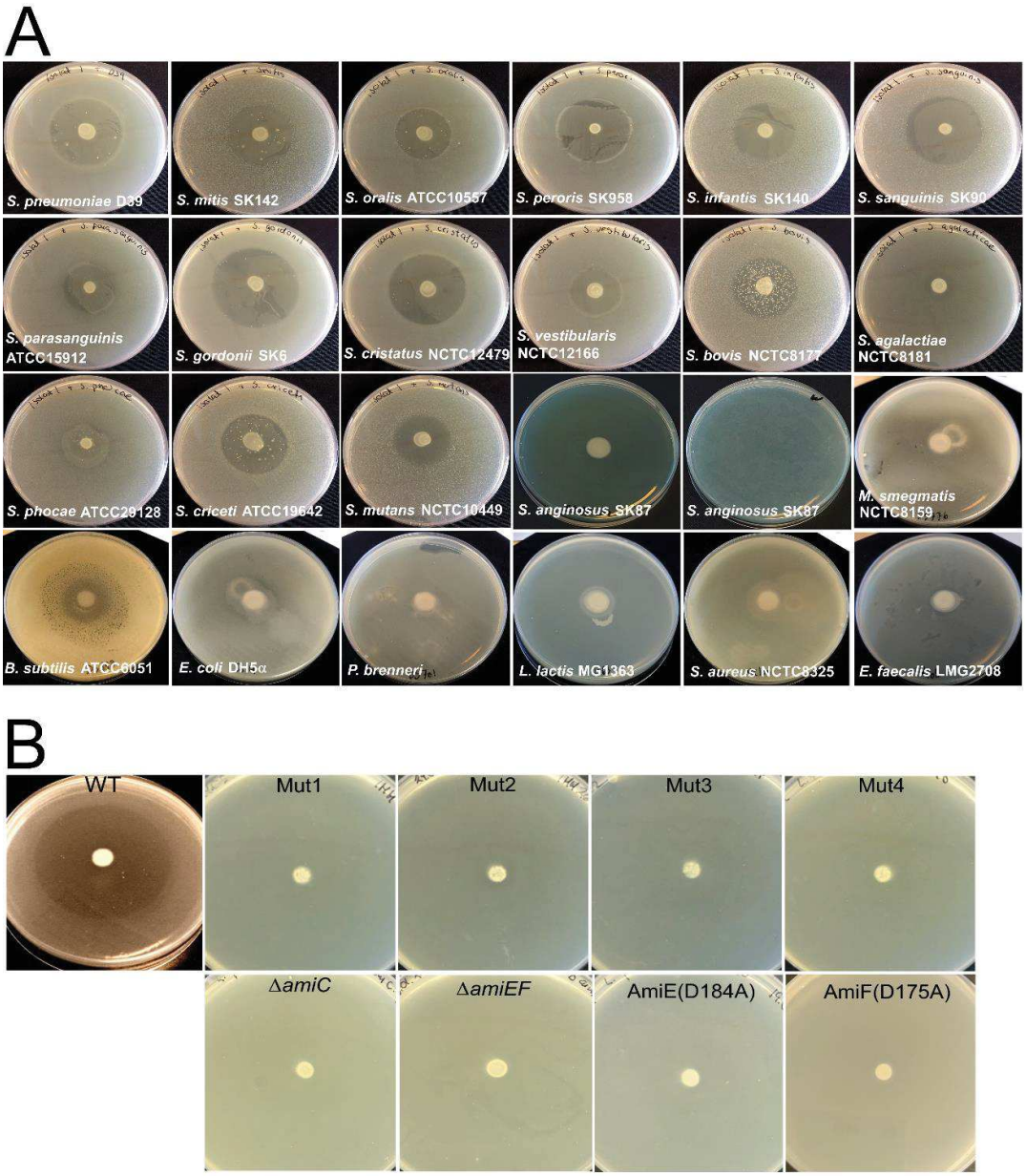

Fig. S4. A. Soft-agar overlays placed on top of two days old *Lysinibacillus* sp. OF-1 spots. Bacteria added to the soft-agar are indicated. *S. criceti* and *S. bovis*, which grew in aggregates in liquid culture, contained several colonies of resistant cells in their inhibition zones, suggesting that cell aggregation could provide protection against lysinicin OF. For some other overlays, e.g., *S. peroris*, *S. gordonii*, *S. sanguinis* and *S. phocae*, *Lysinibacillus* sp. OF-1 had started to migrate into the inhibition zones, which appeared as a grey coating on top of the soft-agar. The inhibition zone of *S. anginosus* covered nearly the whole agar plate, and an overlay without the *Lysinicibacillus* sp. OF-1 spot was included as control of *S. anginosus* growth. **B.** In the upper panels, *S. pneumoniae* mutant 1-4 (spontaneous lysinicin OF resistant mutants) were used as indicator strains, while the lower panels represent overlays containing mutants Δ*amiC*, Δ*amiEF*, $AmiE^{D184A}$ and $AmiF^{D175A}$. All pneumococcal mutants were resistant to Lysinicin OF as no inhibition zones were observed around the *Lysinibacillus* sp. OF-1 spots. An overlay containing wild type was included to show a typical inhibition zone.

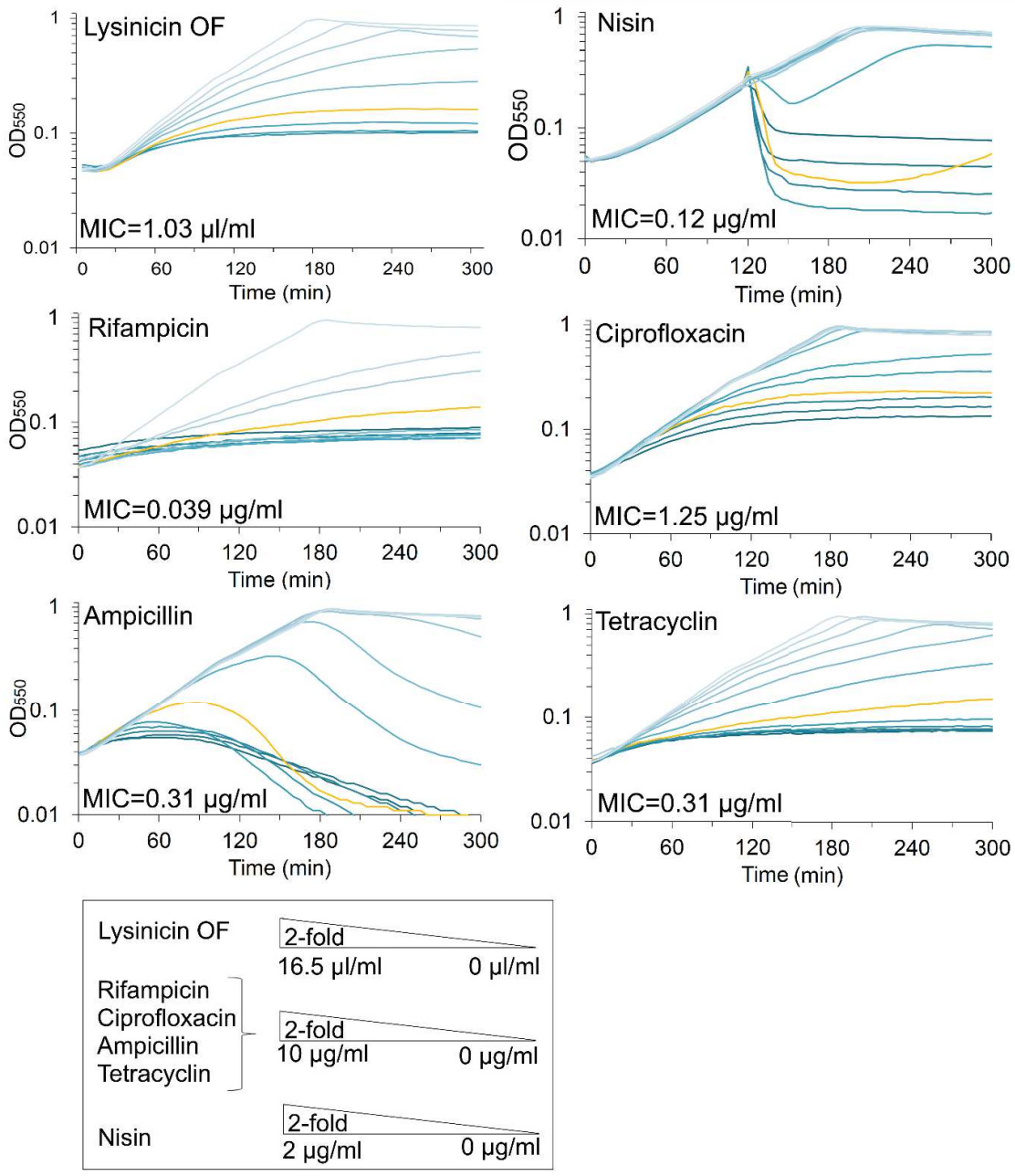

Fig. S5. Estimations of MIC values. *S. pneumoniae* RH425 was grown in the presence of two-fold dilution series of lysinicin OF, rifampicin, ciprofloxacin, ampicillin, tetracycline and nisin. The yellow growth curves were defined as MIC values (indicated in each panel). The dilution series used for each antimicrobial are shown at the bottom left.

Fig. S6. Multiple sequence alignment of AmiE, AmiF and DppD (PDB 4FWI). The conserved Walker A and Walker B motifs are shown in green and yellow, respectively. The aspartic acid residue involved in coordination of a Mg^{2+} ion is boxed (D184 in AmiE and D175 in AmiF).

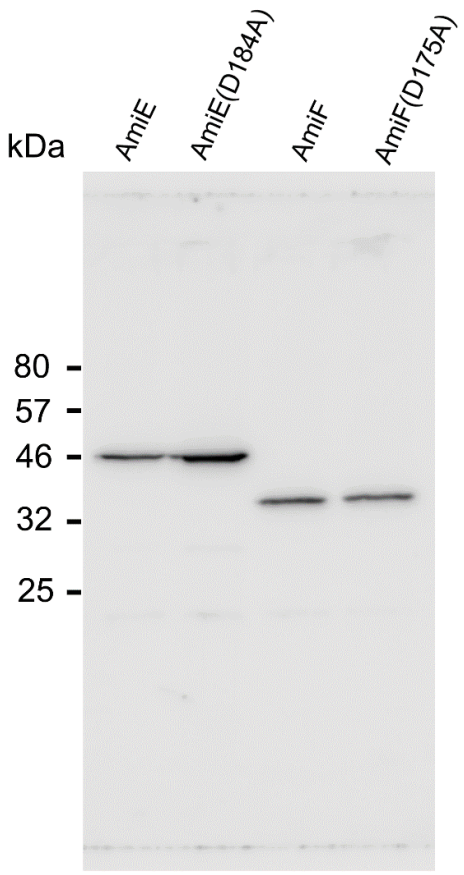

Fig. S7. The D184A and D175A mutations did not reduce the stability of AmiE and AmiF in *S. pneumoniae*. Immunodetection of C-terminally Flag-tagged AmiE, AmiF and their D184A and D175A counterparts in whole cell extracts. The genes were expressed from their native loci. Exponentially growing cells from 5 ml cultures were collected at OD_{550} = 0.25 and resuspended in 100 µl SDS sample buffer. The samples were heated at 95°C for 10 min before 15 µl samples were separated in a 12% SDS-PAG and subsequent electroblotting and immunodetection.

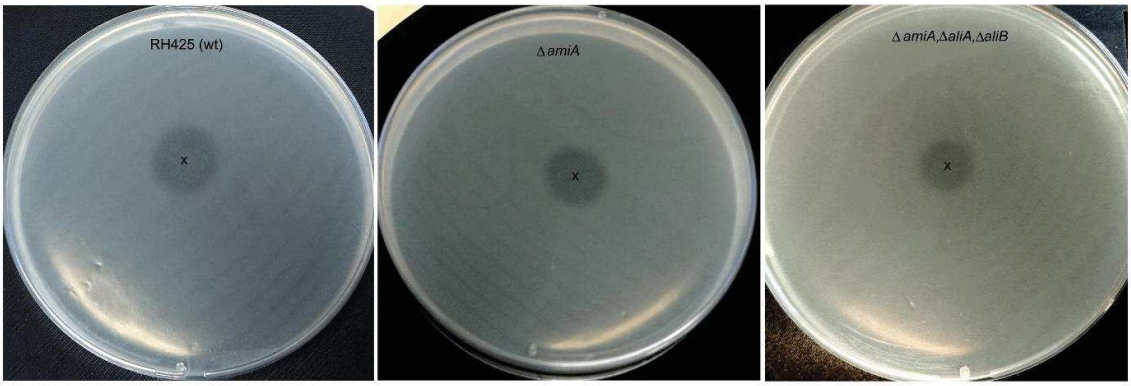

Fig. S8. The Δ*amiA* and Δ*amiA*, Δ*aliA*, Δ*aliB* triple mutants were sensitive to lysinicin OF. Three µl of lysinicin OF was spotted on top of a soft-agar overlay (marked with an x) containing either *S. pneumoniae* RH425, a Δ*amiA* or a Δ*amiA*, Δ*aliA*, Δ*aliB* mutant. Growth inhibition is seen as clear zones in the soft-agar.

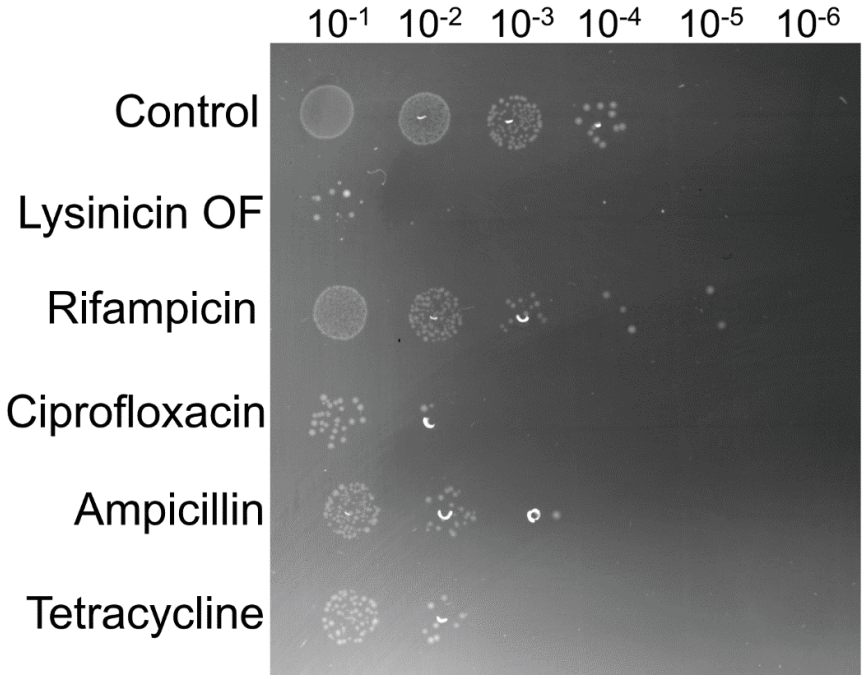

Fig. S9. Spot-assay comparing the survival of lysinicin OF treated *S. pneumoniae* with other antibiotic treatments. Cells were treated for 30 min with 10xMIC of each antimicrobial before antibiotic removal and OD adjustment. The different antibiotics are indicated on the figure left, and the dilution of cell culture on the top. Three µl of each dilution were spotted on TH-agar.

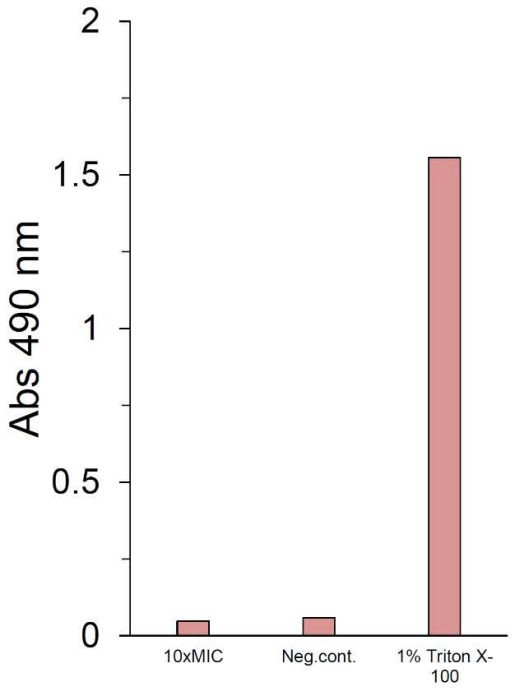

Fig. S10. Lysinicin OF did not cause hemolysis of sheep blood. The absorption at 490 nm in the supernatants of blood samples treated with 10xMIC of Lysinicin OF were compared with supernatants of non-treated blood and blood treated with 1% (v/v) Triton X-100.

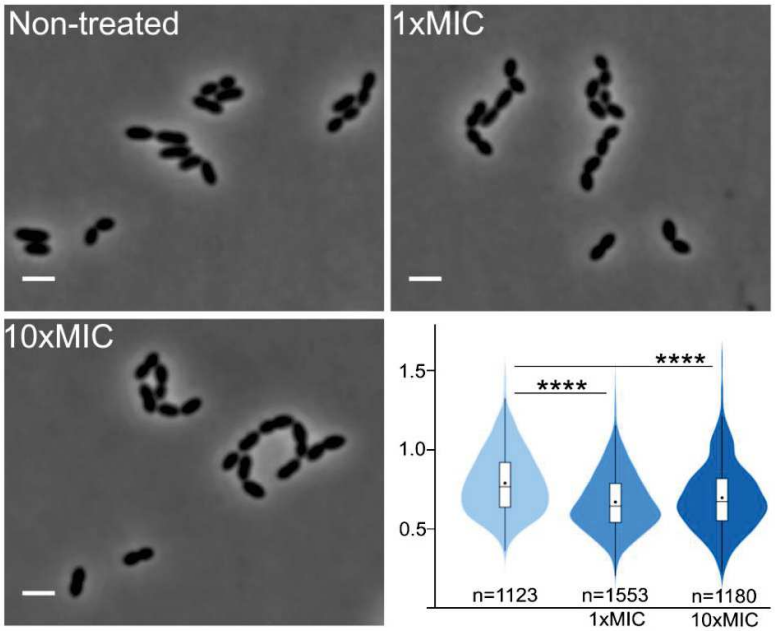

Fig. S11. Concentrations of lysinicin OF corresponding to 1xMIC (1 µl/ml) and 10xMIC (10 µl/ml) was added to *S. pneumoniae* at OD_{550} = 0.1. After four hours at 37°C, cells were imaged by phase contrast microscopy, and the average cell sizes (area in μm^2) were estimated using MicrobeJ, here represented as violin plots. Average cell size ranged from 0.79 ± 0.20 μm^2 (non-treated) to 0.67 ± 0.18 μm^2 (1xMIC) and 0.70 ± 0.21 μm^2 (10xMIC). P values were obtained relative to non-treated cells using one-way analysis of variance (ANOVA). ****, P < 0.00001. Scale bars are 2 µm.

Table S1. Bacterial species used in this study.

***S. pneumoniae* strains**	Relevant characteristics	Source
RH14	R6 derivative, Δ*comA*::*ermAM*, Δ*lytA*::kan; Ery^r, Kan^r	(4)
RH425	R6 derivative, but Δ*comA*::*ermAM*, *rpsL1*; Ery^r, Sm^r	(5)
IHH21	RH425, but Δ*amiC*::janus, Ery^r, Kan^r	This study
IHH22	RH425, but Δ*amiEF*::janus, Ery^r, Kan^r	This study
IHH23	RH425, but *amiE*(D184A); Ery^r, Sm^r	This study
aw495	RH425, but *amiF*(D190A); Ery^r, Sm^r	This study
VS14	RH425, but *amiE-Flag*; Ery^r, Sm^r	This study
VS15	RH425, but *amiE(D184)-Flag*; Ery^r, Sm^r	This study
VS16	RH425, but *amiF-Flag*; Ery^r, Sm^r	This study
VS17	RH425, but *amiF(D175A)*-Flag; Ery^r, Sm^r	This study
ds1024	RH425, but Δ*amiA*::*aad9*; Ery^r, Sm^r, Spc^r	This study
ds1030	RH425, but Δ*amiA*::*aad9*, Δ*aliA*::janus, Δ*aliB*::*cat*; Ery^r, Spc^r, Kan^r, Cm^r	This study
mut1	RH425, but C→T at position 1676261, truncated AmiC; Ery^r, Sm^r	This study
mut2	RH425, but G→A at position 1673543, truncated AmiE; Ery^r, Sm^r	This study
mut3	RH425, but deletion from position 1672934-1674011, truncated AmiE and Δ*amiF*; Ery^r, Sm^r	This study
mut4	RH425, but G→T at position 1673313, truncated AmiF; Ery^r, Sm^r	This study
D39	Wild type	(6)
Other streptococcal species[a]		
S. mitis SK142	Wild type	Lab stock
S. oralis ATCC10557	Wild type	Lab stock
S. peroris SK958	Wild type	Lab stock
S. infantis SK140	Wild type	Lab stock
S. sanguinis SK90	Wild type	Lab stock
S. parasanguinis ATCC15912	Wild type	Lab stock
S. gordonii SK6	Wild type	Lab stock
S. cristatus NCTC12479	Wild type	Lab stock
S. vestibularis NCTC 12166	Wild type	Lab stock
S. bovis NCTC8177	Wild type	Lab stock
S. agalactiae NCTC8181	Wild type	Lab stock
S. phocae ATCC29128	Wild type	Lab stock
S. criceti ATCC19642	Wild type	Lab stock
S. mutans NCTC10449	Wild type	Lab stock

S. angonisus SK87	Wild type	Lab stock
Other bacterial species		
B. subtilis ATCC6051	Wild type	ATCC
M. smegmatis NCTC8159	Wild type	UKHSA
E. coli DH5a	Cloning host	Invitrogen
Pseudomonas brenneri, Norwegian isolate	Wild type	Lab stock, this study
L. lactis MG1363	Wild type	Lab stock
S. aureus NCTC8325	Wild type	Lab stock
E. faecalis LMG2708	Wild type	Lab stock
Lysinibacillus sp. OF-1		This study

[a]Streptococcal lab stocks were kindly provided by Prof. Mogens Kilian.

Table S2. Oligoes used for PCR.

Oligo name	Sequence (5'→3')	Source
Primers used for 16S rDNA amplification		
11F	TAACACATGCAAGTCGAACG	(7)
1492R	GGTTACCTTGTTACGACTT	(8)
Primers used for amplifying the Janus cassette		
Kan484.F	GTTTGATTTTTAATGGATAATGTG	(9)
RpsL41.R	CTTTCCTTATGCTTTTGGAC	(9)
Construction of a Δ*amiC*::janus cassette (used in combination with Kan484.F and RpsL41.R)		
IHH3	AATATCTATTACACACAATCAGG	This study
IHH4	CACATTATCCATTAAAAATCAAACCATGGAGAGAAAGTTCTATTAG	This study
IHH5	GTCCAAAAGCATAAGGAAAGGGTAAAATGTTGATTGACTCTG	This study
IHH6	GGACAAGGATACCAAGACAAGG	This study
Construction of a Δ*amiEF*::janus cassette (used in combination with Kan484.F and RpsL41.R)		
IHH7	TCTAATAACTCTATGGTCGTTG	This study
IHH8	CACATTATCCATTAAAAATCAAACTTCTACTCCTATCTATGTGTAC	This study
IHH9	GTCCAAAAGCATAAGGAAAGTGGTCGTGCTATCATCGGTC	This study
IHH10	TTAGTCCTTTTTGATAACGTGC	This study

Construction of an *amiE* (D184A) cassette (IHH11 and IHH12 were used in combination with IHH7 and IHH 10, respectively).		
IHH11	AGCACAGATCAAGACATCAGG	This study
IHH12	CCTGATGTCTTGATCTGTGCTGAGCCAACAACTGCCTTGG	This study
Construction of an *amiF* (D190A) cassette (IHH13 and IHH14 were used in combination with IHH7 and IHH10, respectively).		
IHH13	AGCTGCAATAACAAAGTCTGGT	This study
IHH14	ACCAGACTTTGTTATTGCAGCTGAGCCAATTTCAGCCTTGGAC	This study
Primers used for C-terminal flag tagging of AmiE (VS15 and VS16 were used in combination with IHH7 and IHH10, respectively)		
VS15	GATTATAAAGATGATGATGATAAATAGGAGGAAGGAAATGTCTGAAAAATTAG	This study
VS16	CTATTTATCATCATCATCTTTATAATCGTCAGCCAGATGGGCAAATCC	This study
Primers used for C-terminal flag tagging of AmiF (VS17 and VS18 were used in combination with IHH7 and IHH10, respectively)		
VS17	GATTATAAAGATGATGATGATAAATAATAATGGTTTTATAATTTCCATGTC	This study
VS18	TTATTTATCATCATCATCTTTATAATCGTTTAGTCCTTTTTGATAACGTGC	This study
Construction of Δ*amiA*::*aad9*		
aad9 F	GTGAGGAGGATATATTTGAATAC	This study
aad9 R	TTATAATTTTTTTAATCTGTTATTTAAATAG	This study
VS1	CTTTATATTGATACGATTCTGAG	This study
VS4	GTGTTCTTGAAACGAGCCATG	This study
ds794	GTATTCAAATATATCCTCCTCACCAACCCTTTCAACAAGAATGG	This study
ds795	ATTTAAATAACAGATTAAAAAAATTATAACTCAAATCAATGGTAAAGATGG	This study
Construction of Δ*aliA*::janus (used in combination with Kan484.F and RpsL41.R)		
Ds802	AAGGCGACGCTAAGCTTGG	This study
Ds803	CACATTATCCATTAAAAATCAAACCTCTCCATTATAGACTCTTTTC	This study
Ds804	GTCCAAAAGCATAAGGAAAGAAAACATGTGAAATAACTGTTGC	This study
Ds805	GCAGCAACACGACTACCTC	This study
Construction of Δ*aliB*::*cat*		
Ds806	TAAGCGTCTCTTGGTTGATAC	This study
Ds807	CCTTTTTTAAAAGTCAATATTACTGTTCCAGAACCTCCTGC	This study
Ds808	GCCTAATGACTGGCTTTTATAAAATCTAATTGTAGATAAGTTTGTG	This study
Ds809	TAGGATTAAGTAATTGAAAGAGG	This study
Cam F	CAGTAATATTGACTTTTAAAAAAGG	This study
Cam R	TTATAAAAGCCAGTCATTAGGC	This study
Primers used for sequencing of the *ami*-locus.		
ds679	TCACTGTAGTCTTTGACACTTC	This study

ds680	CTGAATGAAGAATTCGAAACATC	This study
ds682	AATTGATTTTCAAGCAGGATCC	This study
ds683	TTGGTTCAGCCATGGCTCG	This study
ds684	GATTTCAATGATGTCAGCAAGG	This study
ds685	GTGGAATTTGACGTTCGTGAC	This study
ds686	GATGCTTTTGCCTTGCGTTC	This study
ds687	GCCTTGGACGTTTCTGTACG	This study
ds688	GCTCATACAACAGGATAGTCG	This study
ds691	CCCAAAGTCCAACCATGACC	This study

Table S3. Different bacteria's sensitivity to lysinicin OF and identity of their AmiC homologues relative to the R6 AmiC

Species	Sensitive	% identity to R6 AmiC	Source
S. pneumoniae R6	Yes		J.P. Claverys
S. pneumoniae D39	Yes	100	(6)
S. mitis SK142	Yes	74 (ATCC 903)[a]	M. Kilian
S. oralis ATCC10557	Yes	92	M. Kilian
S. peroris SK958	Yes	92	M. Kilian
S. infantis SK140	Yes	93	M. Kilian
S. sanguinis SK90	Yes	81 (ATCC 29667)[a]	M. Kilian
S. parasanguinis ATCC15912	Yes	74	M. Kilian
S. gordonii SK6	Yes	83 (challis)[a]	M. Kilian
S. cristatus NCTC12479	Yes	80	M. Kilian
S. vestibularis NCTC 12166	Yes	77	M. Kilian
S. bovis NCTC8177	Yes	26	M. Kilian
S. agalactiae NCTC8181	No	27	M. Kilian
S. phocae ATCC29128	Yes	65	M. Kilian
S. criceti ATCC19642	Yes	27	M. Kilian
S. mutans NCTC10449	Yes	28	M. Kilian
S. anginosus SK87	Yes	83 (ATCC 12395)[a]	M. Kilian
B. subtilis ATCC6051	Moderate	28	ATCC
M. smegmatis NCTC8159	No	28	UKHSA
E. coli DH5a	No	34	Invitrogen
Pseudomonas brenneri	No	29 (FH4)[a]	Lab stock, This study
L. lactis MG1363	No	33	Lab stock
S. aureus NCTC8325	No	30	Lab stock
E. faecalis LMG2708	No	34 (ATCC 29212)[a]	Lab stock

[a] Indicates the strain used to for comparison with the pneumococcal AmiC sequence.

References.

1. Koumoutsi A, Chen XH, Henne A, Liesegang H, Hitzeroth G, Franke P, et al. Structural and functional characterization of gene clusters directing nonribosomal synthesis of bioactive cyclic lipopeptides in *Bacillus amyloliquefaciens* strain FZB42. J Bacteriol. 2004;186(4):1084-96.
2. Hsiao TL, Revelles O, Chen L, Sauer U, Vitkup D. Automatic policing of biochemical annotations using genomic correlations. Nat Chem Biol. 2010;6(1):34-40.
3. Eichenberger P, Fujita M, Jensen ST, Conlon EM, Rudner DZ, Wang ST, et al. The program of gene transcription for a single differentiating cell type during sporulation in *Bacillus subtilis*. PLoS Biol. 2004;2(10):e328.
4. Eldholm V, Johnsborg O, Haugen K, Ohnstad HS, Håvarstein LS. Fratricide in *Streptococcus pneumoniae*: contributions and role of the cell wall hydrolases CbpD, LytA and LytC. Microbiology (Reading, England). 2009;155(Pt 7):2223-34.
5. Johnsborg O, Håvarstein LS. Pneumococcal LytR, a protein from the LytR-CpsA-Psr family, is essential for normal septum formation in *Streptococcus pneumoniae*. J Bacteriol. 2009;191(18):5859-64.
6. Slager J, Aprianto R, Veening JW. Deep genome annotation of the opportunistic human pathogen *Streptococcus pneumoniae* D39. Nucleic Acids Res. 2018;46(19):9971-89.
7. Edwards U, Rogall T, Blocker H, Emde M, Bottger EC. Isolation and direct complete nucleotide determination of entire genes. Characterization of a gene coding for 16S ribosomal RNA. Nucleic Acids Res. 1989;17(19):7843-53.
8. Weisburg WG, Barns SM, Pelletier DA, Lane DJ. 16S ribosomal DNA amplification for phylogenetic study. J Bacteriol. 1991;173(2):697-703.
9. Johnsborg O, Eldholm V, Bjørnstad ML, Håvarstein LS. A predatory mechanism dramatically increases the efficiency of lateral gene transfer in *Streptococcus pneumoniae* and related commensal species. Mol Microbiol. 2008;69(1):245-53.